THERMAL DIFFUSION OF ASYMMETRIC HYDROGEN MOLECULES IN INERT GASES

J. VAN DE REE

THERMAL DIFFUSION OF ASYMMETRIC HYDROGEN MOLECULES IN INERT GASES

THERMAL DIFFUSION OF ASYMMETRIC HYDROGEN MOLECULES IN INERT GASES

PROEFSCHRIFT

TER VERKRIJGING VAN DE GRAAD VAN DOCTOR IN
DE WISKUNDE EN NATUURWETENSCHAPPEN AAN
DE RIJKSUNIVERSITEIT TE LEIDEN, OP GEZAG VAN
DE RECTOR MAGNIFICUS DR P. MUNTENDAM,
HOOGLERAAR IN DE FACULTEIT DER GENEESKUNDE,
TEN OVERSTAAN VAN EEN COMMISSIE UIT DE SENAAT
TE VERDEDIGEN OP WOENSDAG 25 OKTOBER 1967
TE 16 UUR

DOOR

JACOBUS VAN DE REE

geboren te Nice (Frankrijk) in 1934

1967
"BRONDER-OFFSET" ROTTERDAM

PROMOTOR : PROF. DR J. KISTEMAKER

Dit werk heeft plaatsgevonden onder de leiding van
Dr J. Los and Dr A.E. de Vries.

The work in this thesis was part of research program of the Stichting voor Fundamenteel Onderzoek der Materie (Foundation for Fundamental Research on Matter) and was made possible by financial support from the Nederlandse Organisatie voor Zuiver-Wetenschappelijk Onderzoek (Netherlands Organisation for the Advancement of the Pure Research).

πολοῦντες γιγνώσκουσιν
(Aristoteles)

Aan mijn ouders
Aan mijn vrouw

VOORWOORD

Teneinde te voldoen aan de wens van de Faculteit der Wiskunde en Natuurwetenschappen volgt hier een kort overzicht van mijn studie.

Nadat ik in 1952 het einddiploma Gymnasium-B aan het Christelijk Lyceum te Zeist had behaald, begon ik mijn studie aan de Vrije Universiteit te Amsterdam. In 1956 deed ik candidaatsexamen in de Wis- en Natuurkunde (F) en in 1962 doctoraal examen met hoofdvak Scheikunde en bijvak Natuurkunde. Een groot deel van mijn wetenschappelijke vorming heb ik te danken aan Prof. Dr. G.J. Hoijtink. Van 1957 tot 1960 heb ik onder leiding van Dr. W.P. Weyland en Dr. P.H. van der Meij, meegewerkt aan het molecuulspectroscopisch onderzoek van de ionen van aromatische verbindingen. In diezelfde tijd heb ik Dr. H.C. Hamers geassisteerd bij de metingen met radioactief jodium als tracer, in het geneeskundig onderzoek aan de P. van Foreestkliniek. Van 1960 tot 1963 was ik leraar in de Natuur- en Scheikunde aan de Christelijke H.B.S. te Zaandam. In februari 1963 aanvaardde ik een benoeming als wetenschappelijk medewerker aan het F.O.M.-Instituut voor Atoom- en Molecuulfysica te Amsterdam, onder de algemene leiding van Prof. Dr. J. Kistemaker. Dit proefschrift is een neerslag van het aldaar verrichte onderzoek. Sinds october 1967 ben ik als wetenschappelijk medewerker verbonden aan de afdeling voor Molecuulfysica van de Technische Hogeschool te Eindhoven.

CONTENTS

INTRODUCTION

There have been many excellent review articles on diffusion [1]) and thermal diffusion [2]) of molecules in mixtures of gases. We, therefore, feel, that it is not necessary to give a broad introduction on the subject. Thermal diffusion appeared to be very sensitive to the characteristics of the collision process and the intermolecular potential.

Experimentally, the thermal diffusion data already available concern predominantly isotopic mixtures of molecular gases, for instance of hydrogen [3,4]) and of carbon monoxyde [5]). Because of the relative simplicity of the description of a collision between an atom and a molecule, we thought it useful to examine mixtures of molecular and atomic gases. Apart from the early measurements of Clusius and Flubacher [6]) of argon and HCl isotopes, no systematic research on this subject appeared to be present in literature. The first part of this thesis has been devoted to the investigation of the thermal diffusion factors of all possible mixtures between inert gases and hydrogen isotopes. The temperature range was chosen so as to have no temperature dependence of the thermal diffusion factor.

Apart from some subtile differences [7]), the theory of Chapman and Enskog [8]), using a spherically symmetric interatomic potential, succeeds very well in predicting transport properties of symmetrical molecules. They behave approximately like atoms. The anomalous behaviour of a group of molecules, which have in common an asymmetric distribution of the atomic masses, therefore is very interesting. The experimental thermal diffusion factors for these molecules depart so far from the calculated values that it was a challenge for many authors to find an answer to this problem. Wang Chang, Uhlenbeck and De Boer [9]) developed a formal kinetic theory for transport properties, which includes the existence of internal degrees of freedom and inelastic collisions. New collision integrals were introduced. Monchick, Yun and Mason [10]) extended this theory to mixtures.

Waldmann [11]) and McCourt and Snider [12]) removed the restriction from the Wang Chang - Uhlenbeck theory, that it did not account for the possible degeneracy of the internal states. This is the case for the rotational energy levels of hydrogen. Although being of great theoretical significance, these advances failed to give the required improvement in the few calculations, which were performed with simplified models. The theoretical formulae still grow in complexity. The second part of this thesis is an attempt to give a reason for the theoretical failures and a contribution to a more adequate calculation of the thermal diffusion factors of asymmetric molecules.

CHAPTER 1

THE POTENTIAL MODEL FOR HYDROGEN - INERT GAS INTERACTION IN THERMAL DIFFUSION

1.1 INTRODUCTION

Both in equilibrium and in non-equilibrium processes isotopic substitution in the molecules has a detectable, although often small effect, which has to be ascribed to variations in the intermolecular potentials and transfer of energy between internal and external degrees of freedom. Due to the different averaging procedures for each process, characteristic changes in the potentials may show up in a different magnitude. The thermal diffusion factor of gaseous mixtures has the advantage of being very sensitive to the potential model, more than to the magnitude of the parameters for a given model. As compared to other transport properties the experimental deviations may be very large, especially when the masses of the two components do not differ much.

The theoretical treatment is simpler for a mixture of a mono-atomic and a poly-atomic gas, than for two gases consisting of poly-atomic molecules. This fact determined our choice to the experimental investigation of the thermal diffusion factors of mixtures of the inert gases and hydrogen isotopes. The hydrogen isotopes offer the possibility of a variation over a wide range of relative mass differences and of molecular asymmetry in the atomic mass distribution. The thermal diffusion factor being in first approximation linear in the relative molecular mass differences of the two components, it is possible to investigate both the case of equal masses and the case of very large separations in changing from ^{3}He and ^{4}He to Ar and Kr.

1.2 EXPERIMENTS WITH ^3He AND ^4He

The thermal diffusion factors were measured in a swing separator [13]. This apparatus multiplies the elementary effect by the number of gas tubes contained between the hot upper part and the cold lower part of the device. The upper side could be varied between 100 °C and 500 °C, whereas the lower part was kept at room temperature. After the stationary state was reached, the separation was measured by analyzing samples of the gas mixtures from the hot and the cold ends of the device. The mixtures which contained the radioactive isotope tritium T, were analyzed with ionization chambers. The other samples were analyzed by mass spectrometry. We confined ourselves to mixtures where the hydrogenic components were in trace concentrations, never becoming larger than 5 %. The total pressure was kept at 200 Torr. Under these circumstances collisions between the hydrogenic molecules occur so rarely, that their effect on the separation can be overlooked. For the same reason it was possible to measure two isotopes of hydrogen at one time, provided they did not interfere with each other in the detection stage. The principle of handling a ternary mixture as two binary mixtures was proved to be sound by Van der Valk and Laranjeira [13].

In treating hydrogenic gases two specific difficulties were encountered. First, hydrogen penetrates rather deeply into metal walls, due to bond formation and diffusion through the solid state as a proton gas. It is, therefore, difficult to remove after a run has been finished. The probability exists that it may perturb following runs. The apparatus must be thoroughly pumped and flushed out with some neutral gas, for instance the carrier noble gas. If not, through exchange reactions at the high temperature walls, the gas may be contaminated with the wrong kind of hydrogen molecules and one might be deceived by an apparently low separation. Second, the separation of the radioactive component T can be too high, due to the formation of heavy water with traces of oxygen, again at the high temperature walls, which act as a catalyst. The activity is then carried by a far heavier molecule, which concentrates on the cold side. Also the background of the ionization chamber is raised by adsorption of active water. In our apparatus the water molecules are frozen out in a liquid air trap, which does not interfere with the thermal diffusion process.

We chose our ternary mixtures always in a way so that the non - radioactive hydrogen isotope was in excess with respect to the very small concentration of the radioactive molecules. Because of its concentration the former prevented the

latter disappearing too rapidly from the mixture due to water formation. Above 500 °C more than 10 % of the hydrogen disappeared in one day, the time necessary to reach a stationary state. Only T_2 could not tolerate another hydrogen carrier, because of the possibility of exchange reactions. It could, therefore, only be measured up to 250 °C. $^4He - D_2$ could be measured on the mass spectrometer by increasing the resolution. Although the resolution was not high enough to discern between ^3He and HD, it was nevertheless possible to measure samples of the mixture by making use of the difference in the ionization potentials. By decreasing the electron energy to 20 Volts, the He^+ signal disappeared and only the HD^+ current was detected.

In the stationary state of a binary mixture the thermal diffusion factor is defined by

$$\alpha = - \frac{T \operatorname{grad} n_1}{n_1 n_2 \operatorname{grad} T} ; \quad n_1 + n_2 = 1, \tag{1.1}$$

where n_1 and n_2 are the mole fractions of the two components and T is the absolute temperature. To avoid complications as to whether the heavier or the lighter component enriches at the cold side, we decided to determine the sign of the thermal diffusion factor by always taking the atomic component as the second. Rewriting the equation (1.1) and inserting $n_2 \approx 1$ for the noble gas component which is in bulk concentration :

$$\operatorname{grad} \ln n_1 = - \alpha \operatorname{grad} \ln T, \tag{1.2}$$

which upon integration becomes

$$\ln q = \ln \frac{(n_1)_H}{(n_1)_C} = - \int_C^H \alpha(T) \, d \ln T = - \alpha \ln \frac{T_H}{T_C}, \tag{1.3}$$

where the subscripts H and C stand for the hot and the cold side of the gas volume. The last step in (1.3) holds when α does not depend on temperature. The separation factor q is also introduced. The slope of the graph of ln q against $\ln T_H/T_C$ yields the thermal diffusion factor α. Fig. 1.1 and 1.2 are two examples of such graphs, with a line drawn through the points, obtained by a least squares fit. Fig. 1.1 gives the experimental points collected in four runs with mass spectrometer analysis. Fig. 1.2 gives two runs with detection in ionization chambers. Both lines go through the origin within the statistical er-

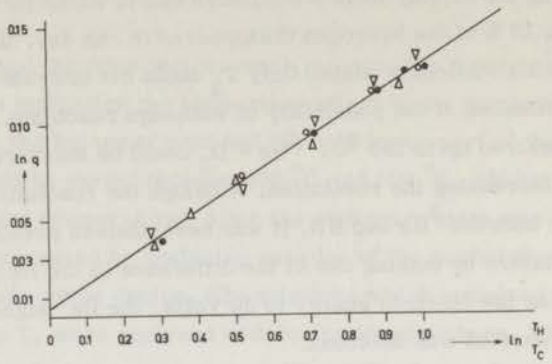

Fig. 1.1 Thermal separation, ln q, of H_2 - ^4He mixture as a function of temperature (Eq. 1.3). For each separate run different symbols are used. Analysis by mass spectrometer.

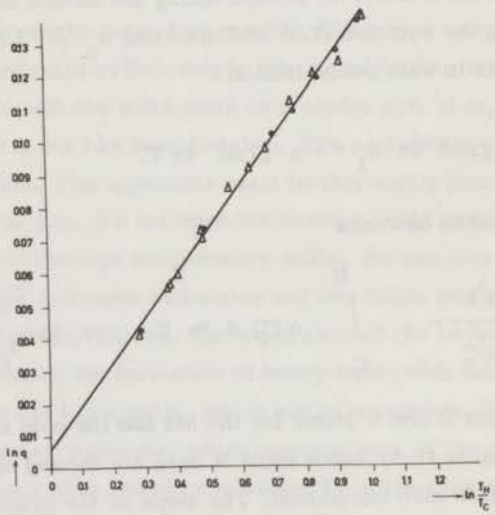

Fig. 1.2 Thermal separation, ln q, of DT - ^3He as a function of temperature (Eq. 1.3). For each separate run different symbols are used. Analysis with ionization chambers.

ror, as they should, because no separation occurs when there is no temperature difference.

1.3 DISCUSSION OF THE EXPERIMENTS

None of the mixtures measured showed any temperature dependence of the thermal diffusion factor in this temperature range. Thus we could assign one value to the thermal diffusion factor α, according to equation (1.3). In Fig. 1.3 and 1.4 the data are plotted for the different mixtures against the relative molar mass differences $(M_1 - M_2) / (M_1 + M_2)$ of the two components. This independent variable has some theoretical background as the thermal diffusion factors that we calculated with the Chapman - Enskog theory for mixtures in which the mass of one of the components may be varied with isotopic substitution, can be approximated by

$$\alpha = c \frac{M_1 - M_2}{M_1 + M_2} + d \qquad (1.4)$$

This result is comparable with Waldmann's [14]) for isotopic mixtures. c and d are numbers which are dependent on the potential model and the temperature at which the experiments are performed. They are, however, independent of the atomic masses. They no longer change in our temperature range and may, therefore, be seen as constants. If the two components in the thermal diffusion experiment are of the same chemical species, the constant d vanishes. The agreement of the experimental points for the symmetric hydrogen molecules with formula (1.4) is very good. The values of c and d are given in TABLE 1.4 for the symmetric molecules.

The experiments show a significant discrepancy between the behaviour of the symmetric and the asymmetric molecules, indicating some additional effect with a negative sign. The deviations of the asymmetric molecules in isotopic CO_2 [15]), CO [5]) and H_2 [3,4]) mixtures could be described reasonably well by a formula derived by Schirdewahn et al. [3]) on basis of a dimensional analysis

$$\alpha = C_M \frac{M_1 - M_2}{M_1 + M_2} - C_\Theta \frac{\Theta_1 - \Theta_2}{\Theta_1 + \Theta_2}, \qquad (1.5)$$

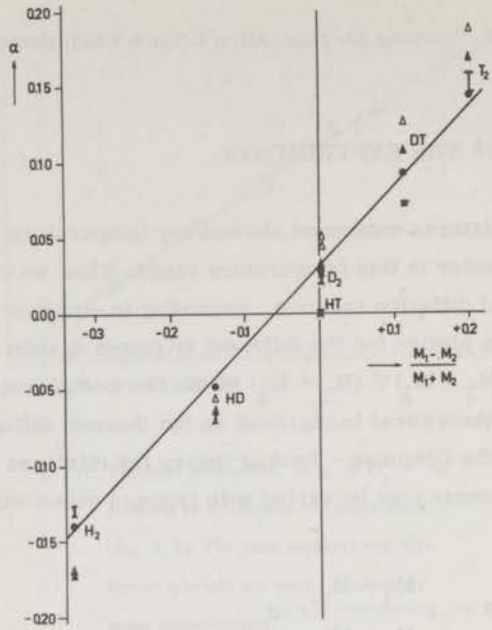

Fig. 1.3 Thermal diffusion factors of the hydrogen isotopes in ^4He, as a function of the relative molecular mass differences. Theoretical calculations : ● , Buckingham exp.-6 potential; ▲ , Lennard-Jones potential; △ , Kihara core potential; I , experimental points. The theoretical points are averages of the values over the temperature range concerned.

TABLE 1.1.

Thermal diffusion factors of the hydrogen isotopes in ^4He (4.0039)

Isotopes	Molecular weight	$\frac{M_1 - M_2}{M_1 + M_2}$	$\alpha_{exp.}$	$\alpha_{theor.}$			
				Lennard-Jones	Buck. exp.-6	Kihara core	α according to formula (1.7)
H_2	2.0163	- 0.330	- 0.129 ± 0.003	- 0.171	- 0.1396	- 0.169	- 0.141
HD	3.0228	- 0.140	- 0.067 ± 0.005	- 0.063	- 0.0485	- 0.056	- 0.059
D_2	4.0294	+ 0.003	+ 0.023 ± 0.002	+ 0.032	+ 0.0305	+ 0.044	+ 0.035
HT	4.0251	+ 0.003	+ 0.000 ± 0.001	+ 0.032	+ 0.0298	+ 0.049	+ 0.003
DT	5.0317	+ 0.114	+ 0.0723 ± 0.001	+ 0.107	+ 0.0921	+ 0.126	+ 0.080
T_2	6.0339	+ 0.202	+ 0.152 ± 0.006	+ 0.168	+ 0.1437	+ 0.187	+ 0.141

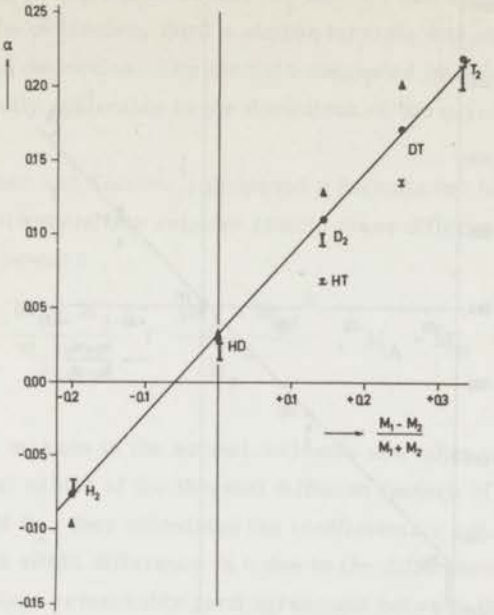

Fig. 1.4 Thermal diffusion factors of the hydrogen isotopes in ^{3}He. (Legend, see Fig. 1.3).

TABLE 1.2.

Thermal diffusion factors of the hydrogen isotopes in ^{3}He (3.0169)

Isotopes	Molecular weight	$\frac{M_1 - M_2}{M_1 + M_2}$	$\alpha_{exp.}$	$\alpha_{theor.}$		
				Lennard-Jones	Buck. exp.–6	α according to formula (1.7)
H_2	2.0163	- 0.199	- 0.071 ± 0.004	- 0.097	- 0.077	- 0.078
HD	3.0228	+ 0.001	+ 0.021 ± 0.006	+ 0.031	+ 0.029	+ 0.011
D_2	4.0294	+ 0.144	+ 0.096 ± 0.002		+ 0.110	+ 0.112
HT	4.0251	+ 0.143	+ 0.068 ± 0.001	+ 0.128	+ 0.110	+ 0.075
DT	5.0317	+ 0.250	+ 0.135 ± 0.002	+ 0.202	+ 0.171	+ 0.155
T_2	6.0339	+ 0.333	+ 0.206 ± 0.008		+ 0.219	+ 0.217

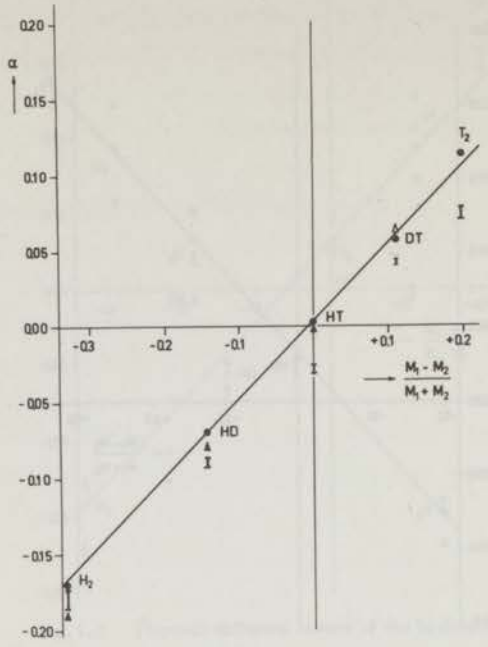

Fig. 1.5 Thermal diffusion factors of the hydrogen isotopes in D_2, gathered from literature (Legend, see Fig. 1.3).

TABLE 1.3.

Thermal diffusion factors of the hydrogen isotopes in D_2.

Isotopes	Molar weight	$\frac{M_1 - M_2}{M_1 + M_2}$	$\alpha_{exp.}$	α theor.		
				Lennard-Jones	Buck. exp.-6	α according to formula (1.7)
H_2	2.0163	- 0.333	$- 0.179 \pm 0.007$ [16]	- 0.190	- 0.171	- 0.177
HD	3.0228	- 0.143	$- 0.090 \pm 0.004$ [29]	- 0.080	- 0.070	- 0.097
D_2	4.0294	0	0	0	0	+ 0.004
HT	4.0251	- 0.000	$- 0.028 \pm 0.002$ [3]	+ 0.000	+ 0.0023	- 0.027
DT	5.0317	+ 0.111	$+ 0.042 \pm 0.002$ [3]	+ 0.063	+ 0.057	+ 0.050
T_2	6.0339	+ 0.199	$+ 0.074 \pm 0.004$ [4]		+ 0.123	+ 0.112

where C_M and C_Θ are constants, and Θ_1 and Θ_2 are the moments of inertia of the two isotopic molecules. Such a simple formula was not derived for mixtures of atoms and molecules. The formula suggested by Schirdewahn [3] in this case, is not directly applicable to the deviations of the asymmetric molecules.

Reichenbacher and Klemm [4] proposed a formula for isotopic mixtures, based on the development into relative atomic mass differences in the molecule. Up to the second power :

$$\alpha = c\,\frac{M_1 - M_2}{M_1 + M_2} - f\,\frac{(M_A - M_B)^2}{M_1^2}\quad,\quad M_A + M_B = M_1 \qquad (1.6)$$

where the atomic masses in the second molecule are taken to be equal. From their experimental values of the thermal diffusion factors of some hydrogen isotopes in H_2 and D_2, they calculated the coefficients c = 0.429 and f = 0.112.

Apart from a slight difference in c due to the differences in the interaction potentials, there is a remarkably good agreement between the measurements in ^{4}He and the set of values which could be gathered from literature, measured in D_2 (Fig. 1.5). To a first approximation, it is, therefore, not an essential feature of the problem, that the second component is a symmetric molecule or an atom. The deviations of the asymmetric molecules in the two series may be compared.

There are some remarks to be made concerning TABLE 1.3. The accuracy is not everywhere the same. Some values were only given for mixtures of rather large concentrations of the hydrogen isotopes and had to be extrapolated to trace concentrations. The value of $T_2 - D_2$ from Reichenbacher and Klemm [4] may be too low due to exchange reactions. This statement is justified by the good agreement we obtained with the theoretical value both with ^{3}He and ^{4}He. Even in this case it was not easy to avoid exchange reactions, because the glass and metal walls are always contaminated with hydrogen. The apparatus had to be saturated with T_2 before the experiment was done and the T_2 had to be drawn directly from a metal container. Of course the same precautions had to be observed in handling D_2, but the concentrations could be taken higher. We took the value of the thermal diffusion factor for $H_2 - D_2$ from Slieker [16], because the measurement was recently done in a swing separator in this laboratory, giving $\alpha = -0.179 \pm 0.007$, in good agreement with the theoretical calculations (TABLE 1.3). Murphey's value of 0.149 ± 0.003 [17] is probably too low.

TABLE 1.4.

Values of the constants c and d from formula (1.4) for the symmetric hydrogen isotopes.

Hydrogen isotopes H_2, D_2 and T_2	experimental value of α		theoretical value of α (Buck pot)	
	c	d	c	d
against ^4He	0.521	0.037	0.530	0.034
against ^3He	0.517	0.029	0.556	0.032
against D_2	0.537	0.000	0.543	0.004

We thought it justified to take the experimental slope c only from the thermal diffusion factors of H_2 - D_2 and D_2 - D_2, which is of course, zero. Thus, we obtain a value for c of 0.537 instead of Reichenbacher's 0.429 (TABLE 1.4).

Then, the deviations predicted by the correction term in (1.6) for the asymmetric molecules HD, HT and DT, being resp. 0.012, 0.028 and 0.005, disagree even with the measurements in D_2. The close resemblance between the deviations in D_2 and ^4He, and the difference with ^3He, indicate a dependency on M_2. The magnitude of the deviations is such that it has to be linear in the atomic mass differences in the molecule. The experiments can better be described by the following formula, which is an extension of Eq. (1.4):

$$\alpha = c\,\frac{M_1 - M_2}{M_1 + M_2} + d - \frac{e}{2}\left|\frac{M_A - M_B}{M_1 + M_2}\right| \qquad (1.7)$$

where e is a constant number. The formula is restricted to mass differences which are not too large. It represents not only the experimental points in ^3He and ^4He, but also those in D_2, when the latter is considered as an atom, which is certainly allowed in this order of approximation. The thermal diffusion factors obtained with (1.7) are listed in the last columns of TABLES 1.1, 1.2 and 1.3. The constants c and d were the theoretical values of TABLE 1.4, from a Chapman - Enskog calculation with a Buckingham exp.-6 potential. For the constant e we used the experimental value 0.258. We may conclude from the value of e that the correction term is linear in the displacement of the center of

mass of the colliding system, due to the asymmetry of the molecule,

$$\frac{M_A - M_B}{M_1 + M_2} \frac{\rho}{2},$$

where ρ is the internuclear distance in the molecule. But also that it is linear in the ratio $\rho/\sigma = 0.74/2.87$, where σ is the collision diameter, rather than the quadratic dependence calculated by Trübenbacher [18]) with the rough spheres model.

1.4 THEORETICAL CALCULATIONS

On statistical considerations Enskog and Chapman [8]) developed a theory for the evaluation of the transport coefficients in gases of low density. They assumed only binary elastic collisions between the molecules. The gradients which are present as driving forces have to be so small as to be able to linearize the hydrodynamic equations for the fluxes. They derive formulae for the transport coefficients in terms of a postulated spherically symmetric potential model for the molecular interaction during the collision. The first approximation to the thermal diffusion factor developed by Kihara [19, 20]), is used here rather than the original Chapman and Cowling approximation. Besides its relatively simpler form, it has the advantage of being closer to the convergence value in its first step than the next order approximation of Chapman and Cowling [21]). For trace concentrations of the first component, labelled 1, which we shall take to be the hydrogenic isotope in all cases, the formula reads :

$$\alpha_T = - \frac{(6\,C^* - 5)\,M_{21}}{2\left[3M_{12}^2 + M_{21}^2 + \frac{8}{5}\,M_{21}\,M_{12}\,A^*\right]} \times$$

$$\left[1 - \left(\frac{M_{12}}{2}\right)^{\frac{3}{2}} \frac{\Omega_{12}^{(2.2)^*}}{\Omega_2^{(2.2)^*}} \frac{\sigma_{12}^2}{\sigma_2^2} \left\{8 + \frac{15}{A^*}\left(\frac{M_{12}}{M_{21}} - 1\right)\right\}\right] \qquad (1.8)$$

where $M_{12} = \frac{M_1}{M_1 + M_2}$ and $M_{21} = \frac{M_2}{M_1 + M_2}$ express the relative molecular weights. The other symbols Ω^* , A^* and C^* are reduced collision integrals or ratios of them, as defined by Hirschfelder, Curtiss and Bird [20].

In order to have a comparison with the experimental values, the theoretical thermal diffusion factors were calculated at two different reduced temperatures $T^* = \kappa T / \epsilon = 20$ and 50, and averaged between them. This was done because the theoretical values showed a tendency to fall off slightly with higher temperatures, a feature which was never verified in experiments.

Three kinds of potential models were used in the calculations. Firstly, the Lennard-Jones 12-6 potential :

$$V(r) = 4 \epsilon \left[\left(\frac{\sigma}{r}\right)^{12} - \left(\frac{\sigma}{r}\right)^{6} \right] , \qquad (1.9)$$

which has two parameters. ϵ is the depth of the potential well, and σ is the internuclear separation r at which $V(r) = 0$. Secondly, the modified Buckingham exponential 6 model, which has three parameters :

$$V(r) = \frac{\epsilon}{1 - \frac{6}{s}} \left[\frac{6}{s} \exp \left(s \left[1 - \frac{r}{r_m} \right] \right) - \left(\frac{r_m}{r} \right)^6 \right] , \quad r \geq r_{max} ;$$

$$V(r) = \infty \qquad , \quad r < r_{max} \qquad (1.10)$$

Again ϵ is the depth of the potential well, r_m is the value of r at this minimum and s is the steepness of the repulsive part of the potential. The Kihara core potential [22]

$$V(r) = 4 \epsilon \left[\left(\frac{1 - \gamma}{\frac{r}{\sigma} - \gamma} \right)^{12} - \left(\frac{1 - \gamma}{\frac{r}{\sigma} - \gamma} \right)^{6} \right] \qquad (1.11)$$

is a Lennard-Jones potential, where a hard core of diameter $\gamma\sigma$ has been introduced, within which the potential is infinity. It has also 3 parameters.

TABLE 1.5.

Potential parameters used for the theoretical calculation of the thermal diffusion factors of the hydrogen isotopes. The same set was used for all isotopes, except for the Kihara core potential.

Gas	Lennard-Jones 12 - 6 potential		Mod. Buckingham exp.-6 potential			Kihara core potential
	$\epsilon/\kappa(^{\circ}K)$	$\sigma(\mathring{A})$	$\epsilon/\kappa(^{\circ}K)$	$r_m(\mathring{A})$	s	γ
H_2	37.00	2.928	37.3	3.337	14.0	0.222
He	10.22	2.576	9.16	3.135	12.4	0.000
mixture	19.45	2.752	18.27	3.244	13.22	

As a starting point we chose the parameters of the Buckingham potential for the individual components, as they were calculated by Mason and Rice [23]) from the second virial coefficient and viscosity data from high temperature experiments. The same authors give also the combining rules for obtaining the parameters of the interaction potential of a mixture. Mason [24]) has tabulated the required collision integrals. The corresponding values of the parameters for the Lennard-Jones potential were found by taking the previous values of the Buckingham potential for the individual components. The parameter is then calculated from the r_m values at each value of the steepness parameter s (p. 34 ref. 20). The simpler combining rules :

$$\epsilon_{12} = \sqrt{\epsilon_1 \epsilon_2} \quad , \qquad \sigma_{12} = \frac{\sigma_1 + \sigma_2}{2} \tag{1.12}$$

were used to obtain the mixture parameters. The required collision integrals are also given by Hirschfelder, Curtiss and Bird [20]).

In what concerns the Kihara core potential, the values of the parameter γ were chosen so as to fit the Lennard-Jones value of α for H_2. For D_2 and T_2 the same γ was used. But for the asymmetric molecules HD, HT and DT, some effect of the asymmetry of the molecule may be included. If the molecules rotate fast enough a core may be assumed with a diameter corresponding

TABLE 1.6.

Values of the thermal diffusion factor of the systems H_2 - ^4He and D_2 - ^4He calculated with a Buckingham exp.-6 potential and with different values of the parameters of hydrogen and deuterium.

H_2 - ^4He system	σ(Å)	r_m (Å)	ϵ/κ (°K)	s	α
Mason and Rice [23])	2.9669	3.337	37.3	14.0	0.1396
ϵ - 5 %	2.9669	3.337	35.4	14.0	0.1396
σ + 1 %	2.9966	3.370	37.3	14.0	0.1393
σ - 1 %	2.9372	3.303	37.3	14.0	0.1399
Knaap and Beenakker [7])	2.928	3.293	37.0	14.0	0.1400
D_2 - ^4He system					
Mason and Rice [23])	2.9669	3.337	37.3	14.0	0.03054
σ + 1 %	2.9966	3.370	37.3	14.0	0.03194
σ - 1 %	2.9372	3.303	37.3	14.0	0.02921
Knaap and Beenakker [7])	2.9758	3.347	35.63	14.0	0.03052

to the orbit described by the lightest atom round the center of mass, thus

$\frac{4}{3}\ \gamma_{H_2}$, $\frac{3}{2}\ \gamma_{H_2}$ and $\frac{6}{5}\ \gamma_{H_2}$ respectively. The required collision integrals are given by Barker, Fock and Smith [25]).

1.5 DISCUSSION OF THE THEORETICAL VALUES

The Kihara core model, did not cover the data. The values are too high and the introduced difference between symmetric and asymmetric molecules is too small and has the wrong sign (Fig. 1.3).

From the two other potentials, without exception, the Buckingham potential fits the experimental data best for the symmetric molecules (Fig. 1.3, 1.4, 1.5). This is the more true as it may be shown that the thermal diffusion factor is not

at all sensitive to changes in the potential parameters. In the high temperature range ε could be varied with $\pm$ 5 % without changing the value of the thermal diffusion factor by more than 0.0001. This is because collisions tend to come close to hard sphere collisions. The depth of the potential well is small with respect to the thermal energy. Changes in σ up to $\pm$ 1 % do not appreciably change the values of α (TABLE 1.6). This means that the thermal diffusion factor in this temperature range is more sensitive to the potential model as a whole, especially to the repulsive part. It would have required absurd values of the parameters to fit the potentials to the experimental points, as was done for other transport properties. Knaap and Beenakker [7]) found that the differences between hydrogen and deuterium, amounting to a few percent in second virial coefficients and in polarizabilities, could be consistently expressed in shifts of the parameters $\Delta\varepsilon/\varepsilon = 0.045$ and $\Delta\sigma/\sigma = -0.003$.

Recently, Mason, Amdur and Oppenheim [1]) made the same comparison of second virial coefficients with viscosity and diffusion. By an analysis of other possible sources of deviations, such as inelastic collisions or anisotropy of the potential, they could assign the difference between hydrogen and deuterium unambiguously to a change in the spherical potential by $\Delta\varepsilon/\varepsilon = 0.06$ and $\Delta\sigma/\sigma = 0.008$.

However, Reichenbacher, Müller and Klemm [26]) could not reproduce any measurable difference between H_2 and D_2 in isothermal diffusion experiments. Anyhow, shifts of this order will not show up in thermal diffusion. Therefore, the conclusion seems to be justified that the same spherically symmetric potential may be used for the symmetric molecules H_2, D_2 and T_2. The fact that the behaviour of the thermal diffusion factors of the hydrogen isotopes in D_2 as a second component, is nearly identical to that with respect to ^{3}He and ^{4}He, is another argument supporting that conclusion.

The agreement between theory and experiment for the symmetric molecules shows most clearly in TABLE 1.4, where the values of c and d from equation (1.4), were found by fitting formula (1.4) to the α's calculated with a Buckingham exp. 6 potential.

The second order calculations of the Kihara approximation [24]) yielded only corrections of α by and amount of 0.001 to 0.005 which stays within experimental error.

Deviations due to quantum effects, even with ^{3}He, are not important in

this temperature region. The quantum corrections to the transport collision integrals were calculated by Imam-Rahajoe, Curtiss and Bernstein [27]. Even for the mixture H_2 - ^3He, with a reduced De Broglie wavelength $\Lambda_{12}^* = 2.32$ at $T^* = 20$, the quantities A^* and C^* change only by 0.2 %. This gives a correction to α of 0.0014 or 1.5 %, which lies within experimental error. In diffusion, heat conductivity and viscosity the interference of inelastic collisions has to be taken into consideration. In a first approach only transitions between rotational states may be of importance in the temperature range of our experiments. In heat conductivity the effect appeared to be rather large and gave rise to the so-called Eucken corrections. In diffusion and viscosity the effect is less pronounced. There is a difference between symmetric and asymmetric molecules in that the former requires about 10^2 collisions to have a transition induced, whereas the latter may already be excited after 10 collisions.

In viscosity the effect may be 0.003 and 0.03. In diffusion the effect is much less, probably in the order of 0.001 for both symmetric and asymmetric cases [1]. In thermal diffusion an explanation of the anomalous behaviour of the asymmetric molecules cannot be expected to come from these rotational excitations, according to Monchick, Yun and Mason [10]. If the excitations are of some influence, one would expect a change in the thermal diffusion factor, if the probability of rotational excitation is changed. It is possible to make such a test by making use of the difference in probability for excitation between symmetric and asymmetric isotopic molecules. This was done for $^{15}N_2$ and $^{15}N^{14}N$ [28]. Our experiments provide also an argument of this kind. The occupation numbers of the different rotational energy levels and the excitation probability change markedly from the two ends of our temperature range. Nevertheless, the thermal diffusion factors remained constant within experimental error (Fig. 1.1 and 1.2).

Because of the sensitivity of the thermal diffusion factor to the molecular interaction potential, it seems that the reason for the deviation of the asymmetric molecules has to be sought in the anisotropy of the potential. The collision process itself has to be investigated closer for changes in the scattering angle, and for the effect of inelastic collisions on the distribution of the molecules over energies and angular momenta, due to the excentric position of the centre of mass [4]. It seems encouraging that the assignment of a lower effective mass to the asymmetric molecules sometimes could cover an extended range of thermal diffusion factors [16, 29].

Such a feature lies outside the scope of the Chapman - Enskog formalism,

unless the effect is so small that it may be treated as a perturbation to a method which is already an approximation itself. The asymmetry effect is indeed of second order, because it does not show in diffusion [1, 26]. Very small deviations in diffusion may, however, be important in thermal diffusion, as can be deduced from the recurrency relation [30],

$$6\ C^* - 5 = 2 \left\{ 2 - \left(\frac{\partial \ln D}{\partial \ln T} \right)_p \right\} \qquad (1.13)$$

The derivative of the diffusion coefficient D is usually near 2, so that $(6\ C^* - 5)$ depends on small differences. This implies that small deviations may be still important in the next order approximation.

1.6 EXPERIMENTS WITH Ar AND Kr

In order to check the validity of Eq. (1.7), the experiments were extended to mixtures with the heavy inert gases ($M_2 \gg M_1$), Argon and Krypton. The condensation temperature of these gases being higher than that of He, the liquid air trap had to be thermostated at some 30 degrees above the condensation point. It was, therefore, not always possible to avoid some contamination of the ionization chambers with radioactive water, produced at high temperatures in the thermal diffusion vessel. After each run, therefore, the mixture was allowed to come to equilibrium at room temperature. If then the ionization chambers showed an unequal signal, they were cleaned by heating, washing and pumping. The run was started over again.

The case of a small concentration of a light gas in a bulk of the heavy component, called a Lorentzian mixture, offers a greater risk for concentration dependence of the thermal diffusion factor. Formula (1.8) reduces to

$$\alpha_T = - \frac{1}{2n_2} (6\ C^* - 5) \qquad (1.14)$$

However, within experimental error, no concentration effect was detected in the range $1\ \% < n_1 < 4\ \%$ of the gases HD, D_2 and H_2. Another source of error may arise from the fact that the thermal diffusion factor of these mixtures is still not in the high temperature limit. We are measuring in the range $5 < T^* < 10$. In order to make no mistake in the comparison between the separations of the different mixtures, the set of top - temperatures in the apparatus was chosen to be the same for each run. The results are shown in Fig. 1.6 and Fig. 1.7.

TABLE 1.7.

Thermal diffusion factors of the hydrogen isotopes in Ar (39.944). Potential parameters for Ar: Lennard-Jones, $\sigma = 3.405$ Å, $\epsilon = 122$ °K; Buck. exp.-6, $\sigma = 3.437$ Å, $\epsilon = 123.2$ °K, $s = 14$.

Isotopes	$\frac{M_1 - M_2}{M_1 + M_2}$	$\alpha_{exp.}$	$\alpha_{theor.}$ ($T^* = 8$)	
			Lennard Jones	Buck. exp.- 6
H_2	- 0.9039	- 0.285 ± 0.006	- 0.3206	- 0.2954
HD	- 0.8593	- 0.290 ± 0.004	- 0.3158	- 0.2907
D_2	- 0.8167	- 0.277 ± 0.005	- 0.3105	- 0.2856
HT	- 0.8169	- 0.264 ± 0.003	- 0.3105	- 0.2856
DT	- 0.7762	- 0.229 ± 0.002	- 0.3046	- 0.2799
T_2	- 0.7375	- 0.235 ± 0.003	- 0.2980	- 0.2737

TABLE 1.8.

Thermal diffusion factors of the hydrogen isotopes in Kr (83.80).

Potential parameters for Kr : Lennard-Jones, $\sigma = 3.597$ Å, $\epsilon = 158$ °K; Buck. exp-6, $\sigma = 3.562$, $\epsilon = 158.3$, $s = 14$.

Isotopes	$\frac{M_1 - M_2}{M_1 + M_2}$	$\alpha_{exp.}$	$\alpha_{theor.}$ ($T^* = 6$)	
			Lennard Jones	Buck. exp. - 6
H_2	- 0.9535	0.263 ± 0.005	- 0.3118	- 0.2962
HD	- 0.9310	0.290 ± 0.003	- 0.3097	- 0.2941
D_2	- 0.9091	0.281 ± 0.003	- 0.3076	- 0.2921
HT	- 0.9091	0.278 ± 0.002	- 0.3076	- 0.2921
DT	- 0.8876	0.180 ± 0.004	- 0.3055	- 0.2900
T_2	- 0.8666	0.231 ± 0.006	- 0.3032	- 0.2878

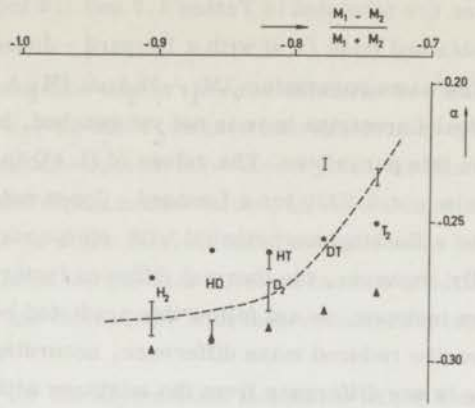

Fig. 1.6 Thermal diffusion factors of the hydrogen isotopes in Argon. (Legend, see Fig. 1.3).

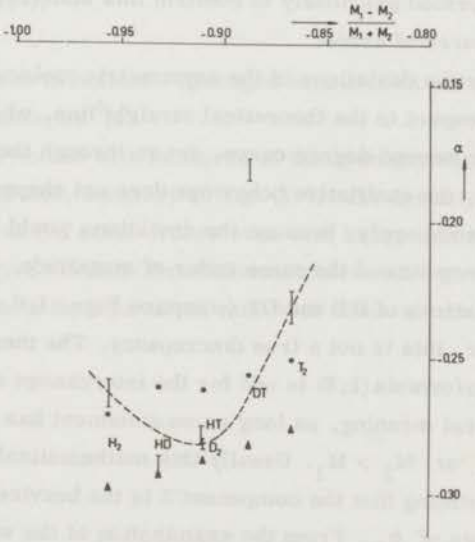

Fig. 1.7 Thermal diffusion factors of the hydrogen isotopes in Krypton. (Legend, see Fig. 1.3).

The numerical values are tabulated in Tables 1.7 and 1.8 together with the theoretical values obtained from (1.8) with a Lennard - Jones and a Buckingham - exp 6 potential. The same parameter $(M_1 - M_2) / (M_1 + M_2)$ was chosen as an abscissa. The ideal Lorentzian case is not yet reached, because there is a small dependence on this parameter. The values of (1.14) in our temperature range are $0.2952 < \alpha_T < 0.3339$ for a Lennard - Jones potential and $0.2763 < \alpha_T < 0.3108$ for a Buckingham potential with steepness 14.

Experimentally, however, the thermal diffusion factors of the different symmetric hydrogen isotopes, do not follow this predicted behaviour, nor the linear dependence on the reduced mass difference, according to the empirical formula (1.4). This is one difference from the mixtures with helium. We have to mention again that the values of T_2 are possibly too low. The set of top - temperatures could not be the same as for the other mixtures. For the moment we have no answer to the question why the symmetric molecules deviate so much from the expected values. We may have traced a difference in the symmetric potentials, which then would appear more distinctly in the case of a Lorentzian gas, because of the strong dependence on every deviation in C_{ij}^*. However, a careful and more accurate investigation of the concentration dependence of α_T must be performed previously to confirm this statement, this being the most important source of error.

Now, whether the deviations of the asymmetric molecules HD, HT and DT are defined with respect to the theoretical straight line, whether this is done with respect to the second degree curve, drawn through the experimental points of H_2, D_2 and T_2, the qualitative behaviour does not change. It is clear that formula (1.7) does not apply, because the deviations would have vanished. The effect, however, remains of the same order of magnitude. There is a reversal of sign in the deviations of HT and DT (compare Figs. 1.6 and 1.7 to 1.3, 1.4 and 1.5). However, this is not a true discrepancy. The thermal diffusion factor α_T, according to formula (1.8) is odd for the interchange of component 1 and 2. This has no physical meaning, as long as no statement has been made about whether $M_1 > M_2$ or $M_2 > M_1$. Usually this mathematical inconvenience is circumvented by stating that the component 2 is the heavier one, obtaining thus only positive values of α_T. From the examination of the whole set of figures, we may now state that HT and DT have a smaller separation, whereas HD has a larger separation compared with the expected value from the calculations with a symmetric potential. Only ^{3}He - HD seems to be an exception to this rule.

1.7 CONCLUSIONS

It could be established that in thermal diffusion in ^3He and ^4He, at high T^* the molecules H_2, D_2 and T_2 behave like spherically symmetric potential centres. The Buckingham exponential-6 model gives the best fit of the Chapman - Enskog theory to the experimental values. In our calculations the shape of the potential appeared to be more relevant that the exact value of the parameters. To a good approximation the thermal diffusion factors are linear in the relative mass differences of the molecules, both theoretically and experimentally (Eq. 1.4).

The deviations for the asymmetric molecules HD, HT and DT could by no means be fitted in the usual Chapman - Enskog theory. Higher order corrections, quantum effects, or inelastic collisions can not be responsible for these deviations. It is felt that the angular dependence of the potential may have an exceptionally large effect in thermal diffusion, which cannot be accounted for by the usual collision integrals. This asymmetry may be correlated with the excentricity of the centre of mass. For small mass differences between the component molecules of the mixture, the deviations are linear in the shift of the centre of mass of the colliding system (Eq. 1.7).

Thermal diffusion in helium - hydrogen mixtures is completely analogous to that of hydrogen isotopes [4].

From the experiments with mixtures of the hydrogen isotopes with Ar and Kr, one can conclude that, contrary to Eq. (1.7), the deviations of the asymmetric isotopes remain of the same order, even with heavy second components. As a rule, HT and DT give smaller separations, whereas HD gives larger separations in comparison with the equivalent case with mono-atomic gases.

CHAPTER 2

CLASSICAL SCATTERING OF AN ATOM FROM AN ASYMMETRIC MOLECULE

2.1 INTRODUCTION

In recent years there has been a considerable theoretical effort to calculate collision cross sections for diatomic molecules involved in inelastic scattering. Special attention has been given to rotational transitions, as they occur in the range of thermal velocities, which is the region most investigated experimentally at present. The need for such calculations is obvious, because of the many anomalies found for molecules in transport properties, sound dispersion and collision broadening of spectral lines.

Advanced computing techniques permit the integration over large numbers of calculated trajectories, since this is the only way of having a test for a proposed interaction potential between particles. This potential manifests itself through a statistical number of collision events.

The quantum mechanical calculations, which start with the Schrödinger equation for the collision problem, suffer from the inaccessibility of the scattering matrices. The solution is usually initiated with a distorted wave approximation, which then limits the range of validity to the weak coupling case, i.e., in general to the lowest rotational transitions or to heavy incident particles [31,32]. There is a second restriction in that the calculations may only be performed for small perturbations of the spherically symmetric potential which governs the interaction between atoms. Usually, for symmetric molecules, the perturbation term arises from the second term in the development of the potential into Legendre polynomials. It contains the angular dependence of the potential in the form

$$V(r, \gamma) = V_0(r) + V_2(r)\ P_2\ (\cos \gamma), \qquad (2.1)$$

where r is the distance between the centres of mass of the particles and γ is the angle between r and the molecular axis (Fig. 2.1). One still has to make an assumption about the values of the expansion coefficients. From first principles, Roberts [33]) performed a theoretical calculation of the potential between He and H_2, restricting himself to the repulsive part. A fit of his numerical topography of the potential field to formula (2.1), which was possible within 3 % error, offered the chance of an evaluation of the quantum mechanical inelastic cross sections of the transition between the lowest rotational levels of H_2. Roberts [33]) and Davison [34]) also calculated the same cross sections in pure hydrogen, based again on a potential of the form (2.1). The reliability of their assumptions and calculations can be examined by the comparison of their results with data on collision numbers. These are obtained from the relaxation times, measured by sound dispersion in gases at low temperatures [35]). The discrepancies established in this way between experiment and theory necessitate an adaption of the development coefficient $V_2(r)$ by over 30 % of its value. Of course, the calculations may suffer from an error by the neglection of the attractive part of the potential, which is important at low velocities.

Cross and Herschbach [36]) performed a classical calculation which at least has the advantage of being exact. They computed deviations in the elastic scattering angle for the collision of an atom and a diatomic symmetric molecule with an angular dependent potential of the form (2.1). However, the results which they communicated are too poor to allow a comparison with other theories or with experiments, or to evaluate cross sections. Moreover, in a classical calculation the necessity of an approximation like (2.1) decreases, so that such a calculation seems extremely well suited to the study of cross sections of a molecule with an asymmetric mass distribution like HD or HT. For such molecules the quantum mechanical approximations fail [31]), because the departure from the spherically symmetric potential is too large to be dealt with by time dependent perturbation methods which have to be applied in the velocity range which is of interest.

The deviations which were found experimentally in thermal diffusion for asymmetric molecules (preceding chapter) greatly exceed the possible results of calculations using some small prolate elongation of the potential. The same may be stated in another way. If one attempts to find parameter values which are able to fit the spherical potential to the experimental data, one surpasses any

reasonable value.

We therefore intend to calculate, using the methods of classical mechanics, the cross sections for transport phenomena and rotational transitions occurring in collisions between ^{4}He and the isotopic hydrogen molecule HT.

2.2. THE ROTATING POTENTIAL MODEL

To a good approximation the intermolecular potential field in gases of homonuclear diatomic molecules can be considered to be spherically symmetric (preceding chapter). The results achieved with such a potential in the theoretical treatment of transport properties indicate only very small deviations from this model. We assume that the intermolecular potential of a molecule with an asymmetric mass distribution, like the isotope HT, does not differ from that of a symmetric one like H_2 or D_2. The interaction is mainly governed by the electron cloud, which is scarcely or not influenced by a change in the mass of the atoms. We stress, however, that the symmetry centre of the potential stays at the geometrical midpoint of the molecule (Fig. 2.1), which rotates at a distance

$$\delta = \frac{m_1 - m_3}{m_1 + m_3} \quad \frac{\rho}{2}$$

from the centre of mass and perpendicular to the angular momentum of the molecule. If the diatomic molecule, with atomic masses m_1 and m_3 and internuclear distance ρ, is considered to be a rigid rotator, this distance δ is fixed. The interaction potential is then represented by the full generating function, as compared to (2.1) :

$$V(r,\gamma) = V(R) ; \tag{2.2}$$

$$\vec{R} = \vec{r} + \vec{\delta} ; \quad R^2 = r^2 + \delta^2 - 2 r \delta \cos \gamma. \tag{2.3}$$

For V (R) we can choose a Lennard - Jones 12-6 potential (1.9)

$$V(R) = 4\epsilon \left(\frac{\sigma^{12}}{R^{12}} - \frac{\sigma^6}{R^6} \right) \tag{2.4}$$

where ε is the depth of the potential well and σ is the intermolecular distance at which V (R) = 0. For the interaction between He and HT, upon which we focus our attention, the constants are taken from the fit of the potential to experimental data on viscosity (ε/κ = 19.446 ^{o}K, σ = 2.7515 $\overset{o}{A}$). In Fig. 2.2 the variation range of V (r) is plotted for different values of γ. The solid lines are the energies at the same fixed orientation for all distances, the broken line is the spherically symmetric potential, plotted for comparison. We can also choose a Buckingham exponential potential modified with a sixth power attraction for the long range forces (1.10) :

$$V(R) = \frac{\varepsilon}{1 - (6/s)} \left[\frac{6}{s} \exp\left\{ s\left(1 - \frac{R}{R_m} \right) \right\} - \left(\frac{R}{R_m} \right)^{-6} \right] \quad , \quad R \geq R_{max},$$

$$V(R) = \infty \quad , \quad R < R_{max}. \qquad (2.5)$$

Both potentials are realistic models of the interaction over a wide range of velocities. The Buckingham potential is expected to improve the results, because of its better fit to experiments (ε/κ = 18.27 ^{o}K, R_m = 3.244 $\overset{o}{A}$, s = 13.22, from TABLE 1.5).

Since no other forces act except those derivable from the above mutual potential of the three bodies, the centre of gravity of the system moves in a straight line with uniform velocity. After the transformation which eliminates this motion, the system is represented by the equivalent two body Hamiltonian with respect to the centre of mass being at rest. The first body represents the rotator with reduced mass $m_1 m_3/(m_1 + m_3)$. The second representative body with reduced mass $m_2 (m_1 + m_3)/(m_1 + m_2 + m_3)$ moves in the rotating potential field V(R). The magnitude of the total experienced force in the plane of the three particles

$$- \frac{dV}{dR} = \varphi (R) \qquad (2.6)$$

can be separated into a modified acceleration

$$- \frac{\partial V}{\partial r} = \frac{\varphi (R)}{R} (r - \delta \cos \gamma) \qquad (2.7)$$

and a torque

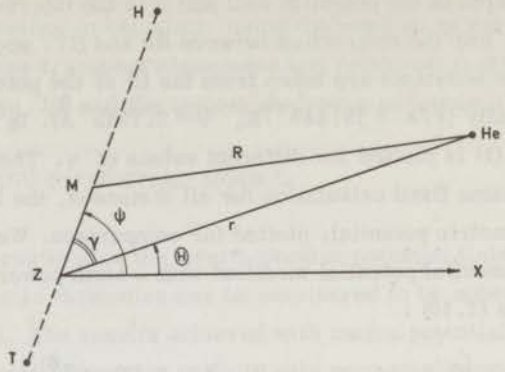

Fig. 2.1 Co-ordinate system for the collision of an atom and a molecule. The diagram shows the plane of the three particles.

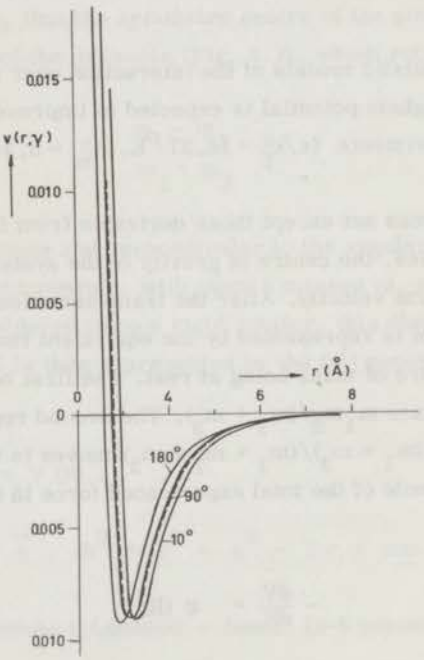

Fig. 2.2 Variation range of the Lennard Jones potential (2.4) for different values of γ. For the system of units we refer to the text. (1 energy unit = $6.557.10^{-3}$ a.u.).

$$-\frac{\partial V}{\partial \gamma} = \frac{\varphi\ (R)}{R}\quad r\ \delta\ \sin\ \gamma. \tag{2.8}$$

The latter may cause the most important correction to the orbit, if the phase of the encounter is such that the molecular axis ρ is perpendicular to the trajectory in the region of closest approach (Fig. 2.3).

2.3 THE EQUATIONS OF MOTION

The most general system of 18 differential equations pertaining to the problem of three bodies, can be reduced to the 6'th order by use of the known invariables of the problem (see for instance Whittaker [37]). Each reduction, using the integrals of motion of the centre of mass, of the angular momentum and of the energy, involves a contact transformation of the initial variables, conserving the Hamiltonian form of the equations. We prefer not to eliminate the total energy H but to introduce the rigid rotator approximation, thereby arriving at a set of 7 differential equations, which read in the Hamiltonian form :

$$\frac{dq_i}{dt} = \frac{\partial H}{\partial p_i}\ ;\ \frac{dp_i}{dt} = -\frac{\partial H}{\partial q_i}\ ;\ (i = 1, \ldots, 4)\ , \tag{2.9}$$

where

$$H = \frac{P_r^2}{2M} + \frac{P_\gamma^2}{2Mr^2} + \frac{(P_\gamma + P_\psi)^2}{2\mu\rho^2} + \left[\frac{\sin^2(\gamma-\psi)}{2\mu\rho^2} + \frac{\sin^2\psi}{2Mr^2}\right]\frac{(k^2 - P_\psi^2)}{\sin^2\gamma} + V\ (R)\ . \tag{2.10}$$

$q_1 = r$, the separation between the centres of mass of the molecule and of the atom.

$q_2 = \gamma$, the angle between ρ and r.

$q_3 = \psi$, a phase angle between ρ and the x-axis.

q_4 is an angle which does not occur in the Hamiltonian and can therefore be ignored, being an angle of the transformation between the x-axes of the moving and the fixed co-ordinate systems. The corresponding integral is k, the total angular momentum, which at infinite separation consists of the rotational angular momentum $\vec{J}$ of the molecule and the orbital angular momentum $\vec{L}$ of the impinging atom.

$$\vec{L} + \vec{J} = \vec{k}. \qquad (2.11)$$

$p_1 = P_r$, the momentum along r.

$p_2 = P_\gamma$, the angular momentum conjugated to γ.

$p_3 = P_\psi$, the angular momentum conjugated to ψ.

$p_4 = k$.

$M = m_2 (m_1 + m_3) / (m_1 + m_2 + m_3)$, the reduced mass of the molecule and the atom.

$\mu = m_1 m_3 / (m_1 + m_3)$, the reduced mass of the molecule.

The co-ordinate system in which the differential equations (2.9) are formulated, was suggested by Cross and Herschbach [36]. It differs from the final co-ordinate system of Whittaker only in that the origin is shifted from its place in one of the particles, to the centre of mass of the molecule and in that polar co-ordinates are used. It is characterized by a z-axis perpendicular to the instantaneous plane of the three particles and it is rotating during the trajectory, the x-axis being the line of nodes with the fixed plane determined by the resultant angular momentum $\vec{k}$ (Fig. 2.4). In quantum mechanics it was also observed that the use of a rotating co-ordinate system can make the computation of cross sections more tractable [38]. The transformed Hamiltonian exhibits separate terms for the contribution of centrifugal and Coriolis forces.

The choice of the initial co-ordinate system is influenced by the necessity of applying an averaging procedure to a multitude of calculated collision patterns. The initial Z-axis will be along the initial angular momentum $\vec{L}$ of the atom. The atom is located in the XY-plane at a distance r from the origin, the centre of mass of the molecule, and at a distance b, called the impact parameter, from the X-axis which is parallel to the initial relative velocity $\vec{g}$. In this co-ordinate system the position of the rotator is determined by its angular momentum vector $\vec{J}$, which has polar angles Θ_J and ϕ_J and by the phase angle ω between the line of nodes of the rotator plane and the molecular axis ρ.

Let p_j^i and q_j^i ($j = 1, \ldots, 6$) be the initial generalized co-ordinates and impulses of the atom and the molecule in this system, then the contact transformation to the fixed co-ordinate system is defined by

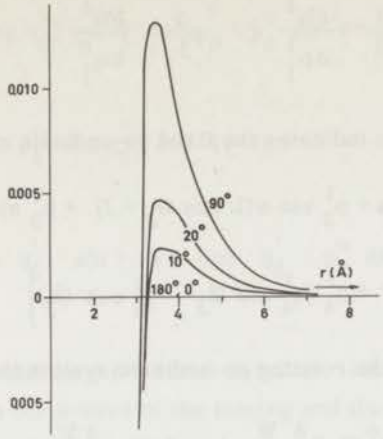

Fig. 2.3 The torque experienced by the motion of the representative body of mass M in the potential field (2.4) at different orientation angles γ.

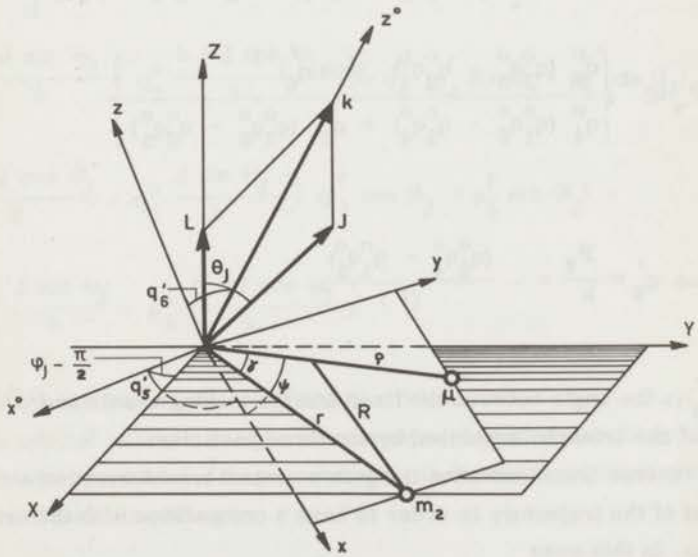

Fig. 2.4 Initial, invariant, and rotating co-ordinate systems pertaining to the three body problem.

$$q_j^i = \frac{\partial W^i}{\partial p_j^i} \; ; \qquad p_j^o = \frac{\partial W^i}{\partial q_j^o} \; , \tag{2.12}$$

where the superscript o indicates the fixed co-ordinate system and where

$$W^i = \frac{\rho}{k} \left[p_1^i \cos \omega + p_2^i \sin \omega (L \cos \Theta_J + J) + p_3^i \sin \omega L \sin \Theta_J \right.$$

$$\left. + p_4^i (q_4^i \sin \Phi_J - q_5^i \cos \Phi_J) \right] \; . \tag{2.13}$$

The transformation to the rotating co-ordinate system then becomes

$$q_j^o = \frac{\partial W}{\partial p_j^o} \; ; \quad p_j = \frac{\partial W}{\partial q_j} \tag{2.14}$$

with

$$W = P_r \, (q_4^{o\,2} + q_5^{o\,2} + q_6^{o\,2}) +$$

$$+ (P_\psi + P_\gamma) \, tg^{-1} \left\{ \frac{q_3^o \, (q_1^o q_5^o - q_2^o q_4^o) \, (\cos q_6')^{-1}}{q_1^o \, (q_1^o q_6^o - q_3^o q_4^o) + q_2^o \, (q_2^o q_6^o - q_3^o q_5^o)} \right\} -$$

$$- P_\gamma \, tg^{-1} \left\{ \frac{q_6^o \, (q_1^o q_5^o - q_2^o q_4^o) \, (\cos q_6')^{-1}}{q_4^o \, (q_1^o q_6^o - q_3^o q_4^o) + q_5^o \, (q_2^o q_6^o - q_3^o q_5^o)} \right\} \tag{2.15}$$

where

$$\cos q_6' = \frac{P_\psi}{k} = - \frac{(q_2^o q_4^o - q_1^o q_5^o)}{0} \tag{2.16}$$

Here q_6' is the angle between the fixed and the moving z-axis and 0 is twice the area of the triangle described by the three particles.

The inverse transformation is again a contact transformation and is applied at the end of the trajectory in order to have a comparison with the original input quantities. In this case

$$W = \rho \left[(p_1^o \cos q_5' + p_2^o \sin q_5') \cos \psi \; - \right.$$

$$- (p_1^o \sin q_5' - p_2^o \cos q_5') \sin \psi \cos q_6' + p_3^o \sin \psi \sin q_6' \Big] +$$

$$+ r \Big[(p_4^o \cos q_5' + p_5^o \sin q_5') \cos (\gamma - \psi) +$$

$$+ (p_4^o \sin q_5' - p_5^o \cos q_5') \sin (\gamma - \psi) \cos q_6' - p_6^o \sin (\gamma - \psi) \sin q_6' \Big] , \tag{2.17}$$

where q_5' is obtained from the differential equation $\partial H / \partial k = dq_4/dt$. q_5' is the angle between the x-axes of the moving and the fixed co-ordinate system. The transformation to the initial, or rather final, co-ordinate system now is achieved by

$$W^f = q_1^o (p_1^f \sin \Phi_J - p_2^f \cos \Phi_J) +$$

$$\left(q_2^o \frac{L + J \cos \Theta_J}{k} - q_3^o \frac{J \sin \Theta_J}{k} \right) (p_1^f \cos \Phi_J + p_2^f \sin \Phi_J) +$$

$$p_3^f \left(q_2^o \frac{J \sin \Theta_J}{k} + q_3^o \frac{L + J \cos \Theta_J}{k} \right) + q_4^o (p_4^f \sin \Phi_J - p_5^f \cos \Phi_J) +$$

$$\left(q_5^o \frac{L + J \cos \Theta_J}{k} - q_6^o \frac{J \sin \Theta_J}{k} \right) (p_4^f \cos \Phi_J + p_5^f \sin \Phi_J) +$$

$$p_6^f \left(q_5^o \frac{J \sin \Theta_J}{k} + q_6^o \frac{L + J \cos \Theta_J}{k} \right) , \tag{2.18}$$

where the superscript f indicates final quantities.

As a special case we want to discuss separately the two-dimensional collision, which occurs when $\vec{J}$ is perpendicular to the XY - collision plane. The Hamiltonian then simplifies to

$$H = \frac{P_r^2}{2M} + \frac{P_\zeta^2}{2Mr^2} + \frac{P_\psi^2}{2 \mu \rho^2} + V(R) \tag{2.19}$$

where $\zeta = \psi - \gamma$. The system of differential equations derived from (2.19) is now of the 6 th order, and is greatly simplified as compared to (2.9). The three moment equations

$$\frac{dP_r}{dt} = \frac{P_\zeta^2}{Mr^3} - \frac{\partial V}{\partial r} ; \quad \frac{dP_\zeta}{dt} = - \frac{\partial V}{\partial \zeta} ; \quad \frac{dP_\psi}{dt} = - \frac{\partial V}{\partial \psi} \tag{2.20}$$

can be reduced using the relationships

$$- \frac{\partial V}{\partial \zeta} = \frac{\partial V}{\partial \psi} = \frac{\partial V}{\partial \gamma} ; \quad k = P_\zeta + P_\psi = Mr^2 \dot{\zeta} + \mu\rho^2 \dot{\psi} , \tag{2.21}$$

where the dots indicate the time derivatives. Then

$$\frac{d}{dt}(\dot{Mr}) = Mr \left(\frac{\mu \rho^2 \dot{\gamma} - k}{\mu\rho^2 + Mr^2} \right)^2 - \frac{r - \delta \cos \gamma}{R} \varphi (R) , \tag{2.22}$$

$$\frac{d}{dt} (\dot{\gamma}) = - 2 \frac{\dot{r}}{r} \left(\frac{\mu\rho^2 \dot{\gamma} - k}{\mu \rho 2 + Mr^2} \right)^6 - \left(\frac{1}{\mu\rho^2} + \frac{1}{Mr^2} \right) \frac{\delta \sin \gamma}{R} \varphi (R) . \tag{2.23}$$

These second order differential equations are similar to the equations for a pendulum with quadratic or with viscous damping. In the attractive range of the potential there is a motion of the rotator towards small angles γ, whereas in the repulsive part the opposite motion is induced.
The deviation of the scattering angle χ ,

$$\cos \chi = - \frac{p_4^f}{p^f} , \tag{2.24}$$

and the excitation or de-excitation of the rotator, resulting from this oscillatory movement, are strongly dependent on the collision time, that is on the time spent in the region where the potential has a significant value. It also depends on the position of the axis ρ during this time, this being a function of the initial phase angle ω. Finally, the angular momentum is most important as it determines the sign of the angular momentum transfer between the two collision partners. For instance, at large velocities g, most of the collision time is spent in the repulsive region of the potential. Then, if $\vec{L} \cdot \vec{J} > J^2$, the repulsion centre

withdraws, the molecule is excited to higher angular velocities $\dot{\psi}$, whereas the scattering angle is smaller as compared to the atom-atom collision. If $\vec{L} \cdot \vec{J} < J^2$, the molecule rotates many times during the collision and imparts a perpendicular motion to the trajectory of the projectile, while it is itself slowing down. Due to the distance δ and the rather large radius of the repulsive core, the change in the scattering angle will persist over a large interval of impact parameters.

In quantum mechanics the limiting cases of very high and very low velocities have their appropriate perturbation treatment, respectively the sudden approximation and the adiabatic treatment. However, in the case we want to examine, i.e. the collision of He on HT at velocities which occur in thermal gases, one may easily evaluate that the rotational period is of the same order as the collision time. The deviations will appear to be so large as to nearly exclude a perturbation treatment. This argument makes a classical calculation preferable, at least as long as a suitable quantum mechanical theory has not been worked out for the scattering of a particle from an oscillating potential. The full development of such a theory has been an object of research for many years. There is a wide range of application in the treatment of the interaction between electromagnetic radiation and matter.

The validity of the classical treatment may be estimated from the requirement that the net momentum transfer $\Delta \vec{p} = \vec{p}^{\,i} - \vec{p}^{\,f}$ has to be much larger than $\hbar/2b$.

$$\Delta p = \left\{ 2M\Delta\epsilon_J + 2Mg^i \left(g^i - g^f \cos\chi\right)\right\}^{\frac{1}{2}} >> \hbar/2b, \qquad (2.25)$$

where $\Delta \epsilon_J = \epsilon_j^i - \epsilon_j^f$ is the energy loss of the rotator in the state j. In our case the classical treatment only breaks down at the lowest velocity, together with impact parameters smaller than 1 $\mathring{A}$.

The same is true for the angular momentum transfer. The quantum mechanical calculations of excitation probabilities [31, 33, 34], thus far concerned H_2 which is a typical quantum gas with respect to the large energy amounts of the rotational jumps. The moment of inertia of HT being much larger than that of H_2, the energy gaps between the levels are much smaller. The jumps with $\Delta j = \pm 1$ are now also more probable (compare $\Delta j = \pm 2$ for H_2). Nevertheless, we are still close to the limit of the applicability of the classical criterion. Only when the energy involved in excitation does not exceed the energy gap between two

levels, the above requirement will be fulfilled. It will be seen from the results of our calculations, that the major part of the asymmetry effect of the HT molecule is to be found already outside the quantum region. We expect that, dealing with heavier molecules, the reliability of the classical cross sections will be improved.

2.4 THE CALCULATIONS

The integration of the differential equations was performed on the EL - X8 computer of the Mathematical Centre of Amsterdam and on the TR-4 computer

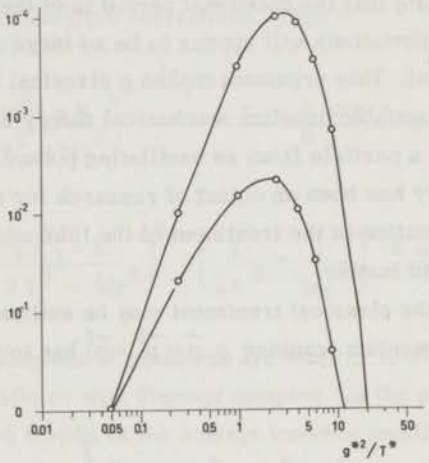

Fig. 2.5 Weight functions $g^{*4}\exp(-g^{*2}/T^*)$ and $g^{*6}\exp(-g^{*2}/T^*)$ at $T^* = 20$.

of the Mathematics Department of the Technical University of Delft. We first performed a comparative test between some integration procedures, a simple step-by-step method, and Adams procedure, a Runge - Kutta procedure and an IBM procedure MILNE (which required 2 secs for the XY-case on the IBM-7094 computer). We chose a fourth-order Runge - Kutta procedure, developed by Zonneveld [39]) in a somewhat more rapid version. In this procedure the independent variable is selected after each integration step in a subroutine which compares the step length to the variable with the maximum change within its particular awarded accuracy. The average time needed for the calculation of one orbit

was about 20 secs for a two-dimensional case (the XY-plane) up to 120 secs for a three-dimensional collision. The input quantities were selected to give a representative set of points in the range of the parameter values of importance. This was done in order to avoid integration over a generated set of random values, which would require more orbits to calculate without giving more information about the details of the collision.

In classical mechanics the rotational energy of a molecule is not discrete. We chose, however, to make use of the knowledge of quantummechanics, introducing as initial values of the angular momentum only those which correspond to the different quantum numbers j. In view of the temperature range of the gases for which we wanted collision integrals with a reasonable accuracy, $T^* = \kappa T/\varepsilon \approx 20$, we confined ourselves to $j = 0, \ldots, 4$ and to initial relative kinetic energies $1 < g^{*2} < 180$, where $g^{*2} = Mg^2/2\varepsilon$ (Fig. 2.5). The variation over the initial phase angle $0^o < \omega < 360^o$ is a typically classical feature of the problem, and as a first step towards a measurable physical quantity, we felt entitled to average over this angle with a variational step of $\Delta\omega = 20^o$. The calculation of the orbit was taken up at a distance $r = 20$ Å, where the input quantities were calculated from the atom-atom scattering of comparable masses. This gave an accuracy in the scattering angle of 0.0005 rad. In order to confine the computing time, we reduced this distance to 10 Å in the three dimensional case, the scattering angle then being accurate to 0.005 rad. The input quantities were transformed from the initial co-ordinate system, described in the foregoing section, by a procedure "enter" to the co-ordinate system of the Hamiltonian (2.10). It is clear from the equations of motion that the system is not invariant under space inversion, due to the asymmetry of the potential (2.2). Therefore, the final scattering angle χ (2.24) cannot be found from

$$\chi = \pi - 2\Theta_m,$$

where Θ_m is the angle between r and the X-axis at the distance of closest approach. This would be true for the case of a central force, such as is usually assumed in the atom-atom collision. In our calculation the orbit has to be followed until the asymmetric interaction is negligible again, i.e. $r = 20$ Å. The resulting values, then, were transformed back to the original centre of mass co-ordinate system by a procedure "exit", and fed again into the equivalent atom-atom collision.

The system of units was also chosen to be suitable for the numerical calculations. In this system the unit of mass is the proton mass, the unit of length

is the Ångstrom = 10^{-8} cm, and the unit of time is 1000 a.u. or 2.4189 . 10^{-14} sec. Then Planck's constant $\hbar = 0.15366$ and Boltzmann's constant $\kappa = 0.4866 . 10^{-3}$. For the particular case of He - HT we used the internuclear distance $\rho = 0.74146$ Å from spectroscopic measurements, $\delta = 0.1854$, $\mu\rho^2 = 0.415578$ and $M = 2.00723$.

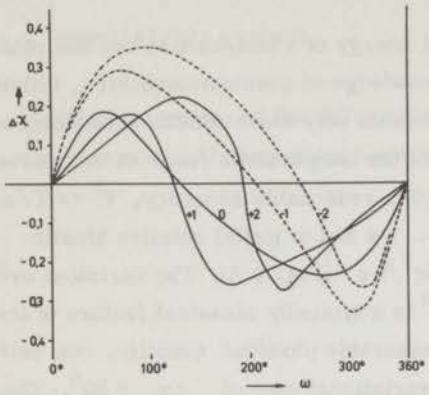

Fig. 2.6 Deviations $\Delta\chi$ (in radians) of the scattering angle ($\chi_o = 1.290$ rad.) as a function of the initial phase angle ω, for initial j = 0, 1 and 2, with orientation of $\vec{J}$ perpendicular to the collision plane. The + sign indicates the configuration $\vec{J}$ and $\vec{L}$ parallel, the -sign stands for anti-parallel. $b^* = 0.727$; $g^{*2} = 20.417$. The curves have been shifted by a phase angle to make them coincide at $\omega = 0^o$. A Lennard Jones potential (2.4) was used.

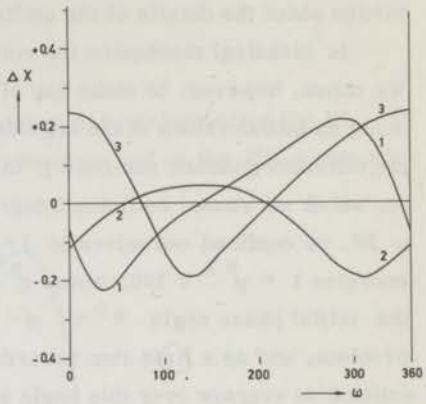

Fig. 2.7 Deviations $\Delta\chi$ (in radians) of the scattering angle ($\chi_o = 1.1523$ rad.) as a function of ω for j = 2. Curve 1 : $\vec{J}$ along Z; curve 2 : $\vec{J}$ along Y; curve 3: $\vec{J}$ along X. $b^* = 0.700$; $g^{*2} = 20$. A Buckingham potential (2.5) was used.

2.5 THE TRANSPORT CROSS SECTIONS FOR INELASTIC SCATTERING

In this section we shall calculate the transport cross sections for the molecule HT in collisions with He. As a consequence of the classical theory every collision is inelastic, showing a smaller or larger amount of exchange between rotational and translational energy. For this reason we use the term "inelastic scattering", which is to be understood as the total scattering arising from both elastic and inelastic collisions. However, in the system He - HT, only a few collisions will reach the necessary amount of energy exchange to be qualified as inelastic in the quantum mechanical sense. This will be shown in the next section.

As for the transport cross sections the average scattering angle over all collisions will be close to the elastic limit. Nevertheless, to take proper account of every contribution to the displacement in the classical scattering theory, we shall use the inelastic formulation of the cross section.

In Fig. 2.6 an example is given of the deviation of the scattering angle χ from χ_o, obtained with $\delta = 0$,

$$\Delta\chi = \chi - \chi_o. \tag{2.26}$$

$\Delta\chi$ is plotted for some initial rotational states, as a function of ω, the initial orientation angle. $\vec{J}$ is along the Z-axis. In Fig. 2.7 $\Delta\chi$ is shown with initial $j = 2$, for different orientations of $\vec{J}$ in space, along the X-, Y- and Z-axes. Because of the torque of the potential (2.8), which behaves like a sine function, we meet a positive and a negative maximum of $\Delta\chi$ in the interval $0 < \omega < 360^o$. As a rule, positive $\Delta\chi$ coincides with de-excitation of the molecule to lower j-states, and, inversely, excitation is coupled with negative $\Delta\chi$. The deviation is seen to depend strongly on ω. The largest contribution to the scattering angle comes from the part of the potential in the region of closest approach. However, the foregoing history of the collision, the pre-orientation in the attractive and the early repulsive part of the potential, strongly influences the phase angle γ. This is seen when the calculation of the orbit is started at distances closer than 10 Å. The true average over all phase angles has, therefore, to be taken with phase angles ω at infinite separation, which all have equal a priori probability.

According to Monchick, Yun and Mason [10]) the collision integrals $\Omega^{(1,1)}$ and $\Omega^{(2,2)}$ for inelastic collisions are extensions of the classical ones for symmetric potentials and without internal states. The possibility of the change of translational energy into internal energy is taken into account by the introduction of the final relative velocity g', which is unequal to g. In the integrands of $\Omega^{(1,1)}$ and $\Omega^{(2,2)}$ the quantities

$$dQ^{(1)} = g^2 (1 - \cos\chi) \tag{2.27}$$

$$dQ^{(2)} = g^4 (1 - \cos^2\chi), \tag{2.28}$$

are changed into

$$dQ^{(1)}_{jm} = g (g - g' \cos\chi) \tag{2.29}$$

$$dQ^{(2)}_{jm} = g^2 (g^2 - g'^2 \cos^2\chi) - \frac{1}{6} (\Delta\epsilon)^2, \tag{2.30}$$

where $\Delta\epsilon = \frac{M}{2}(g^2 - g'^2)$. The subscripts j and m indicate that such an integrand exists for every initial rotational quantum number j, and every magnetic quantum number m. Of course, in our classical calculations, m is no quantum number, but it indicates the projection of $\vec{J}$ on the orbital angular momentum $\vec{L}$ at the onset of the collision:

$$m = J_Z / |\vec{J}| \tag{2.31}$$

Because we are interested in the departure of the molecule HT from the behaviour of a particle with a symmetric potential, we decided to integrate the difference between dQ_{jm} and dQ separately. So we calculated the differences

$$\Delta^{(1)}_{jm} = \left[g^* (g^* - g'^* \cos\chi) - g^{*2} (1 - \cos\chi_o) \right]_{av.} =$$

$$= \left[g^* (g^* \cos\chi_o - g'^* \cos\chi) \right]_{av.} \tag{2.32}$$

$$\Delta^{(2)}_{jm} = \left[g^{*2} (g^{*2} - g'^{*2} \cos^2\chi) - \frac{1}{6} (g^{*2} - g'^{*2})^2 - \right.$$

$$\left. - g^{*4} (1 \cos^2 \chi_o) \right]_{av.}$$

$$= \left[g^{*2} (g^{*2} \cos^2 \chi_o - g'^{*2} \cos^2 \chi) - \frac{1}{6} (g^{*2} - g'^{*2})^2 \right]_{av.} \tag{2.33}$$

The quantities $\Delta^{(1)}$ and $\Delta^{(2)}$ have been averaged over the initial phase angles ω. We remark that we have used $g^{*2} = Mg^2/2\epsilon$, instead of g^2. Most tables of transport cross sections for atom-atom collisions to which we want to compare our results, are computed as a function of this reduced parameter [20].

We next have to integrate the curves over the impact parameters and average over the available m-numbers. Thus, we will obtain the corrections to the transport cross sections $Q^{(\ell)*}$ [20] for each rotational state.

$$\Delta Q^{(\ell)*}_j (g^{*2}) = \left(\frac{2}{\left[1 - \frac{1}{2} \frac{1 + (-1)^\ell}{1 + \ell} \right]} \int_0^\infty \frac{\Delta^{(\ell)}_{jm}}{g^{*2\ell}} b^* \, db^* \right)_{av. over\ m} . \tag{2.34}$$

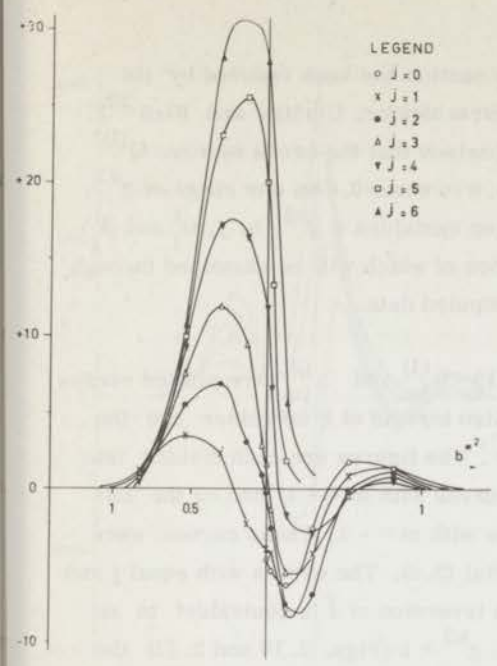

Fig. 2.8 $\Delta^{(1)}_{jm}$ (Eq. 2.32) as a function of impact parameter for different initial rotational states j, averaged over initial phase angles ω. On the left hand side we have m = -1, on the right hand side m = + 1. $g^{*2} = 81.666$.

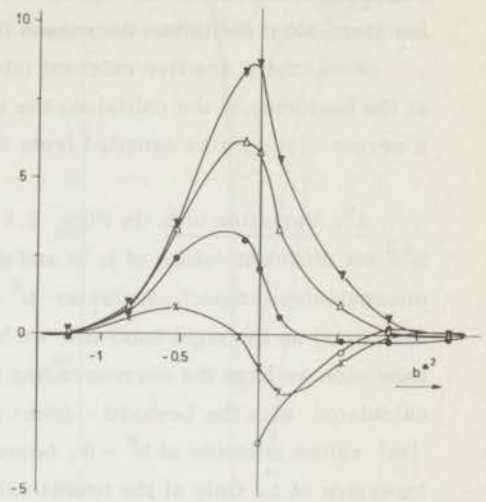

Fig. 2.9 See caption Fig. 2.8; $g^{*2} = 20.417$.

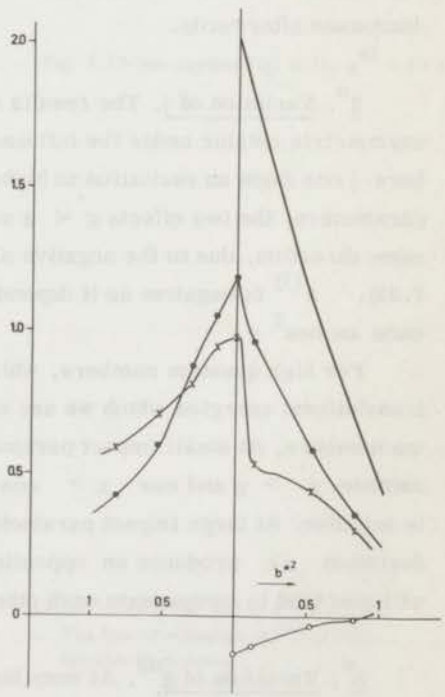

Fig. 2.10 See caption Fig. 2.8; $g^{*2} = 1.021$. The line of reference $dQ^{(1)}$ (2.27) has also been drawn.

The superscript * indicates that the cross section has been reduced by its value for the rigid sphere, as is done by Hirschfelder, Curtiss and Bird [20]. From the same reference we note for comparison that the cross section $Q^{(1)*}$ for atom-atom collisions decreases from 1.0 to about 0.6 in our range of g^{*2}.

Now, there are five relevant integration variables (: g^{*2}, b, j, Θ_j^i and ϕ_j^i) at the beginning of the collision, the influence of which will be examined through a series of diagrams sampled from the computed data.

1°. Variation of b. In Figs. 2.8 to 2.13 $\Delta_{jm}^{(1)}$ and $\Delta_{jm}^{(2)}$ are plotted versus b^{*2} for different values of j, m and g^{*2}. Also instead of b we rather use the dimensionless impact parameter $b^* = b/\sigma$. The figures are each divided into two parts; on the right hand side we have curves with m = + 1, and on the left hand side we have the corresponding curves with m = - 1. These curves were calculated with the Lennard - Jones potential (2.4). The curves with equal j and |m| values coincide at $b^* = 0$, because an inversion of $\vec{J}$ is equivalent to an inversion of $\vec{L}$. Only at the lowest velocity, $g^{*2} = 1$ (Figs. 2.10 and 2.13) the deviations Δ were so large, that it was possible to insert the reference curve dQ, without blowing up the figure. $dQ^{(1)}$ is a decreasing curve with value $dQ^{(1)} = 2\, g^{*2}$ at $b^* = 0$; $dQ^{(2)}$ increases from 0 to a maximum, $dQ^{(2)} = g^{*4}$ and decreases afterwards.

2°. Variation of j. The results demonstrate the physical behaviour of the asymmetric rotator under the influence of the collision. For small quantum numbers j one finds an excitation to higher j-values and therefore, for small impact parameters, the two effects $g' < g$ and $\cos \chi < \cos \chi_0$ both contribute in the same direction, due to the negative sign of the cosine function (Eq. 2.32 and Eq. 2.33). $\Delta^{(1)}$ is negative as it depends on $\cos \chi$; $\Delta^{(2)}$ is positive as it depends on $\cos^2 \chi$.

For high quantum numbers, which have stored energy much larger than the translational energies which we are using, one finds de-excitation to lower quantum numbers. At small impact parameters, the two effects again reinforce one another. $g' > g$ and $\cos \chi > \cos \chi_0$, so that $\Delta^{(1)}$ is positive and $\Delta^{(2)}$ is negative. At large impact parameters the cosine function is positive and the deviation $\Delta\chi$ produces an opposite change in the cosine function. Both effects will now tend to compensate each other.

3°. Variation of g^{*2}. At very high velocities the corrections almost decrease

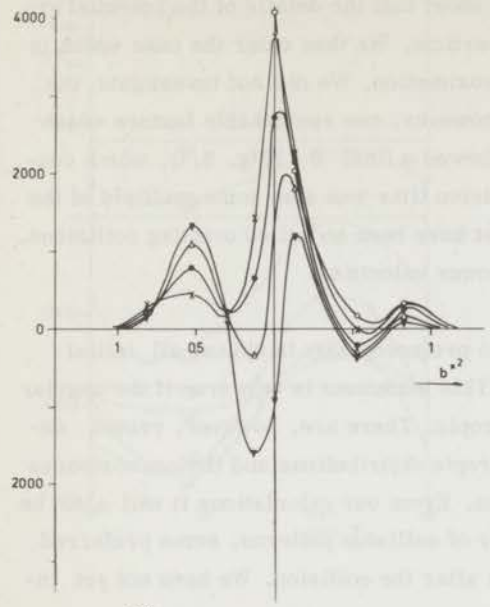

Fig. 2.11 $\Delta^{(2)}_{jm}$ (Eq. 2.33). See caption fig. 2.8. $g^{*2} = 81.666$.

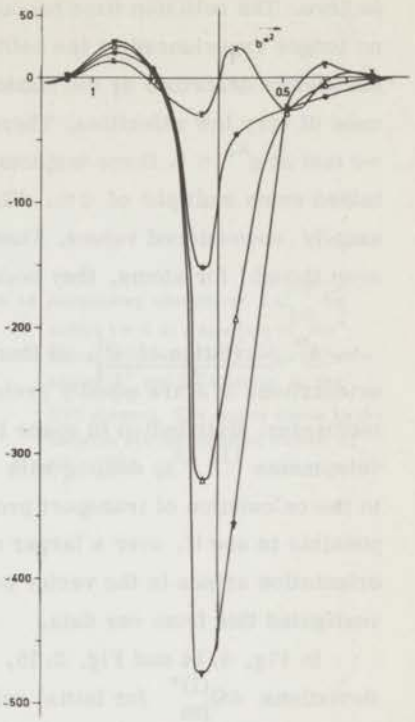

Fig. 2.12 See caption Fig. 2.11. $g^{*2} = 20.417$.

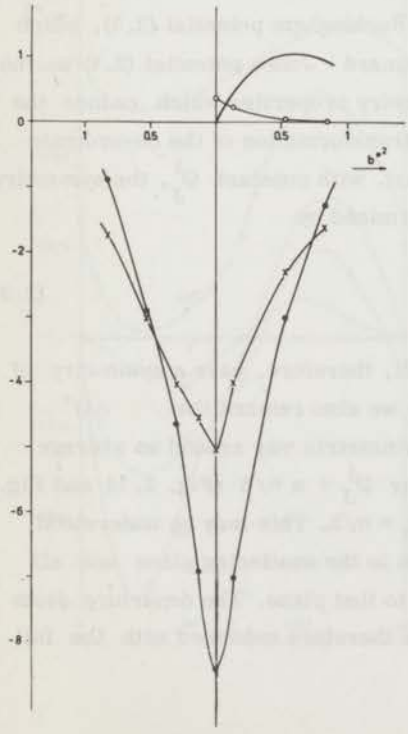

Fig. 2.13 See caption Fig. 2.11. $g^{*2} = 1.021$. The line of reference $dQ^{(2)}$ (2.28) has also been drawn.

to zero. The collision time becomes so short that the details of the potential are no longer experienced by the colliding particle. We then enter the case which is adequately described by the sudden approximation. We did not investigate the case of very low velocities. There is, however, one remarkable feature which we met at $g^{*2} = 1$. Some trajectories showed a final Θ' (Fig. 2.1), which contained some multiple of 2π. The collision time was also some multiple of the usually encountered values. These must have been so called orbiting collisions, even though, for atoms, they occur at lower velocities.

4°. Variation of $\emptyset^i_j$. If there is no preferred axis in space, all initial orientations of $\vec{J}$ are equally probable. This statement is only true if the angular momentum distribution in space is isotropic. There are, however, recent developments [11, 12], dealing with anisotropic distributions and the consequences to the calculation of transport properties. From our calculations it will also be possible to see if, over a larger number of collision patterns, some preferred orientation arises in the vector position after the collision. We have not yet investigated this from our data.

In Fig. 2.14 and Fig. 2.15, and in Table 2.1 and Table 2.2 we show the deviations $\Delta Q^{(1)*}_{jm}$ for initial relative energy $g^{*2} = 20$ and initial rotational quantum numbers $j = 1$ and $j = 2$, respectively. The results of these three dimensional calculations were obtained with a Buckingham potential (2.5), which yielded almost the same ΔQ^* as the Lennard - Jones potential (2.4) in the corresponding cases. There are some symmetry properties which reduce the number of required trajectories. From the transformation of the co-ordinate system (2.13) and (2.16) it can be derived that, with constant Θ^i_J, the symmetry of the scattering angle $\cos\chi$ is mainly determined by

$$\cos^2 \emptyset^i_J - \sin^2 \emptyset^i_J \qquad (2.35)$$

The curves of equations (2.32) and (2.33) will, therefore, have a symmetry of $\emptyset^i_J + n\pi$ ($n = 0, 1, 2 \ldots\ldots$). From (2.35) we also remark that ΔQ^* oscillates as a function of $\emptyset^i_J$ in a nearly symmetric way around an average value, the amplitudes having opposite sign for $\emptyset^i_J + n\pi/2$ (Fig. 2.14 and Fig. 2.15). The oscillations are strongest for $\Theta^i_J = \pi/2$. This may be understood from the observation that the $\vec{J}$ vector is then in the scattering plane and all torque contributions are now perpendicular to that plane. The departure from the spherically symmetric potential model is therefore enhanced with the full

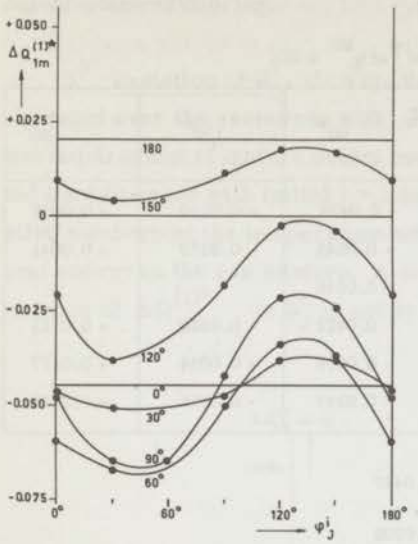

Fig. 2.14 Asymmetry corrections $\Delta Q^{(1)*}_{1m}$ for initial j = 1 as a function of the initial orientation of $\vec{J}$ in space (polar angles φ^i_j and Θ^i_j relative to the XYZ system). The curves shown in the diagram are for different values of Θ^i_j. $g^{*2} = 20$.

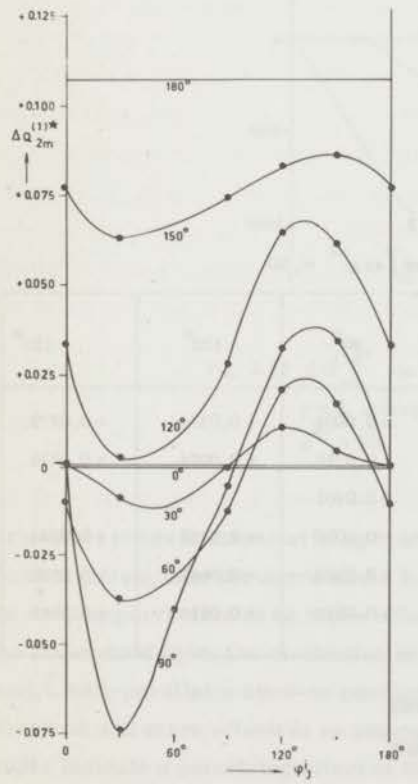

Fig. 2.15 $\Delta Q^{(1)*}_{2m}$ for initial j = 2. See caption Fig. 2.14.

TABLE 2.1.

$\Delta Q^{(1)*}_{1m}$ (in $\mathring{A}^2$). Dependence on the orientation of $\vec{J}$ at $g^{*2} = 20$.

φ^i_J \ Θ^i_J	30°	60°	90°	120°	150°
0°	- 0.0463	- 0.0595	- 0.0478	- 0.0210	+ 0.0095
30°	- 0.0506	- 0.0672	- 0.0648	- 0.0379	+ 0.0041
60°			- 0.0646		
90°	- 0.0475	- 0.0502	- 0.0422	- 0.0183	+ 0.0115
120°	- 0.0382	- 0.0340	- 0.0216	- 0.0024	+ 0.0177
150°	- 0.0378	- 0.0370	- 0.0243	- 0.0038	+ 0.0167

for $\Theta^i_J = 0^\circ$ we have - 0.0447

$\Theta^i_J = 180^\circ$ " " + 0.0202

TABLE 2.2.

$\Delta Q^{(1)*}_{2m}$ (in $\mathring{A}^2$). Dependence on the orientation of $\vec{J}$ at $g^{*2} = 20$.

φ^i_J \ Θ^i_J	30°	60°	90°	120°	150°
0°	+ 0.0004	- 0.0105	+ 0.0004	+ 0.0336	+ 0.0772
30°	- 0.0090	- 0.0372	- 0.0738	+ 0.0024	+ 0.0633
60°			- 0.0401		
90°	- 0.0005	- 0.0128	- 0.0057	+ 0.0285	+ 0.0744
120°	+ 0.0107	+ 0.0215	+ 0.0328	+ 0.0647	+ 0.0832
150°	+ 0.0042	+ 0.0173	+ 0.0348	+ 0.0616	+ 0.0862

for $\Theta^i_J = 0^\circ$ we have - 0.0003

$\Theta^i_J = 180^\circ$ " " + 0.1073

out-of-plane scattering.

5°. Variation of Θ_J^i. In Fig. 2.16 we show the Θ_J^i-dependence of $\Delta Q_{jm}^{(1)*}$ averaged over the variations with Φ_J^i, and weighted with $\sin \Theta_J^i$ in order to meet the requirement of equal a priori probability for every orientation of $\vec{J}$. We selected the two cases with initial j = 1 and j = 2, because they have the highest occupation numbers at the temperature where $g^{*2} = 20$ is the most probable translational energy in the gas mixture. A striking feature in Fig. 2.16 is that the dependence of $\Delta Q_{jm}^{(1)*}$ on Θ_J^i is not symmetric about 90°. The corrections to the

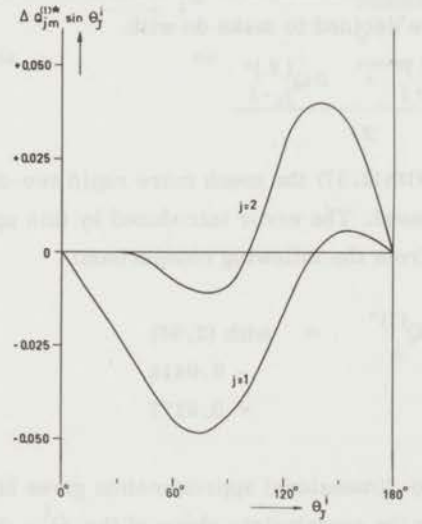

Fig. 2.16 $\Delta Q_{jm}^{(1)*} \sin \Theta_J^i$ for initial j = 1 and j = 2, averaged over the Φ_J^i-values. $g^{*2} = 20$.

transport cross sections arising from negative m-values are more positive (or less negative) than the corrections from positive m-values. The configuration m = - 1 appears also to be more effective in de-excitation than m = + 1. This can be understood from the mechanics of the collision. In the configuration with $\vec{J}$ and $\vec{L}$ anti-parallel a head-on encounter with the rotating potential centre is more frequent and more effective as compared with parallel positions. Thus, our results indicate a polarizing effect of the orientation of $\vec{J}$ on transport or relaxation

phenomena based on inelastic scattering. It becomes of importance as soon as a preferred axis is introduced in space, which may be the direction of the particle velocity in a beam, but a temperature gradient in a gas as well. Therefore, the assumptions of equal probability for $\vec{J}$ - orientation as well as the effect of the collisions on the orientation distribution have to be re-examined.

Because of the very long time used in computing the integration over all $\vec{J}$ - orientations

$$\Delta Q_j^{(\ell)*} = \int_0^{2\pi} \int_0^{\pi} \Delta Q_{jm}^{(\ell)*} \sin \Theta_J^i \, d\Theta_J^i \, d\phi_J^i \qquad (2.36)$$

and because we wanted to have insight in the results of variations over a large range of g^{*2} and j, we decided to make do with

$$\Delta Q_j^{(\ell)*} = \frac{\Delta Q_{j,+1}^{(\ell)*} + \Delta Q_{j,-1}^{(\ell)*}}{2} \qquad (2.37)$$

as an approximation. With (2.37) the much more rapid two-dimensional version of the calculation can be used. The error introduced by this approximation is rather large as may be seen from the following comparison:

$\Delta Q_j^{(1)*}$ =	with (2.36)	with (2.37)
for j = 1	- 0.0414	- 0.0123
for j = 2	+ 0.0177	+ 0.0535

We remark that the two-dimensional approximation gives higher results, because it does not account for the asymmetric shape of the Θ_J^i - dependence. However, from sample calculations we found an improvement for higher j - numbers. Some results of the two-dimensional calculations have already been exhibited in Figs. 2.8 to 2.13 and discussed above. We integrated the curves over the impact parameters according to (2.34) and averaged over the m = + 1 and m = - 1 values according to (2.37). The results are tabulated in Tables 2.3 and 2.4 and shown graphically in Figs. 2.17 and 2.18. For comparison we repeat that the cross section $Q^{(1)*}$ for atom-atom collisions in this range of g^{*2} decreases from 1.0 to about 0.6. (Ref. 20, p. 558). On the average our cross sections are 20% larger. The corrections to the $Q^{(2)*}$ are smaller, about 10 %, except at very low velocities where they reduce the older values by 30 % and more.

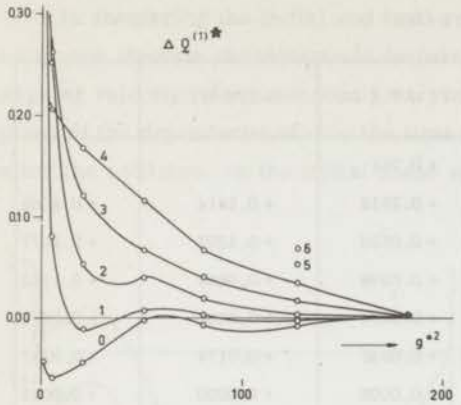

Fig. 2.17 Asymmetry corrections $\Delta Q_j^{(1)*}$ for different initial values of j, as functions of g^{*2} according to (2.37). The reference quantity $Q^{(1)*}$ varies from 1.0 to about 0.6 in this energy range for an atom-atom collision.

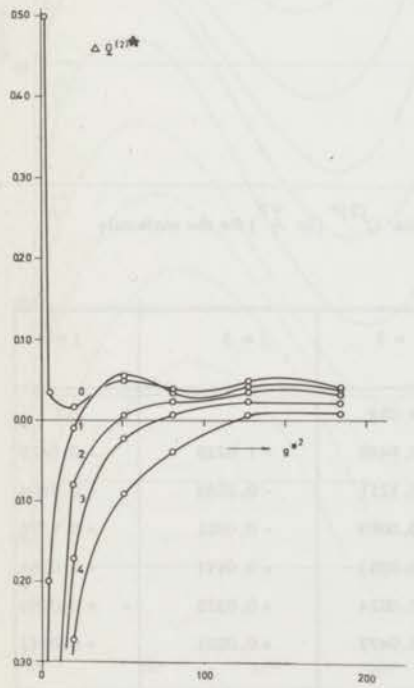

Fig. 2.18 Asymmetry corrections $\Delta Q_j^{(2)*}$ for different initial values of j, as functions of g^{*2} according to (2.37). The values still have to be multiplied with the numerical factor 3/2 occurring in front of the integration (2.34) (Compare Tabel 2.4).

TABLE 2.3.

Asymmetry corrections on the diffusion cross section $Q^{(1)*}$ (in $\mathring{A}^2$) for the molecule HT colliding with ^4He.

g^{*2}	j = 0	j = 1	j = 2	j = 3	j = 4
1.021	- 0.043	+ 0.753	+ 0.761		
5.104	- 0.058	+ 0.0803	+ 0.2518	+ 0.2614	+ 0.2065
20.417	- 0.044	- 0.0112	+ 0.0526	+ 0.1207	+ 0.1677
51.042	- 0.0019	+ 0.0074	+ 0.0398	+ 0.0665	+ 0.1152
81.666	- 0.0068	+ 0.0032	+ 0.0194	+ 0.0402	+ 0.0670
127.60	- 0.0069	- 0.0016	+ 0.0045	+ 0.0174	+ 0.0347
183.75	- 0.0001	+ 0.0001	+ 0.0008	+ 0.0020	+ 0.0033

TABLE 2.4.

Asymmetry corrections on the viscosity cross section $Q^{(2)*}$ (in $\mathring{A}^2$) for the molecule HT colliding with ^4He.

g^{*2}	j = 0	j = 1	j = 2	j = 3	j = 4
1.021	+ 0.748	- 4.735	- 9.039		
5.104	+ 0.0514	- 0.3079	- 0.9466	- 1.0228	- 0.6429
20.417	+ 0.0243	- 0.0158	- 0.1211	- 0.2584	- 0.4104
51.042	+ 0.0743	+ 0.0846	- 0.0089	- 0.0351	- 0.1376
81.666	+ 0.0594	+ 0.0534	+ 0.0353	+ 0.0111	- 0.0584
127.60	+ 0.0750	+ 0.0658	+ 0.0524	+ 0.0355	+ 0.0096
183.75	+ 0.0615	+ 0.0600	+ 0.0473	+ 0.0321	+ 0.0143

2.6 THE CROSS SECTIONS FOR EXCITATION AND DE-EXCITATION

In comparing the initial and final rotational angular velocity of the molecule, one meets a characteristic feature of classical mechanics. That is, the angular velocity is a continuously varying function. In Fig. 2.19 an example is given of the dependence of $\dot{\psi}$, the time derivative of the angle ψ (see Fig. 2.1) after the collision, on the initial phase angle $\psi_{t=0} = \omega$. The curves are given

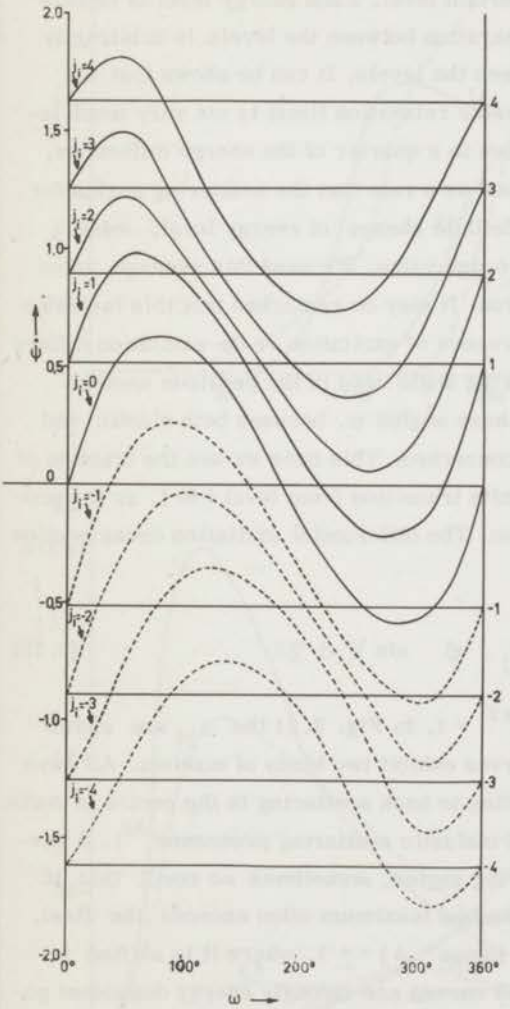

Fig. 2.19 Final rotational angular velocity $\dot{\psi}$ as a function of the initial phase angle ω, for different initial rotational velocities (left hand ordinate) or quantum numbers j (right hand ordinate). See caption of Fig. 2.6.

for different initial values of $\dot{\psi}$, corresponding to quantum numbers $j_i = 0, 1, 2, 3$ and 4. The starting values with $m = -1$ have been indicated by $-1, -2, -3$ and -4. The phases ω of the curves have been shifted in order to have them starting at the same point, $j_f = j_i$. The left hand ordinate is scaled for values of $\dot{\psi}$, the right hand ordinate shows the corresponding j values. The curves are seen to be nearly symmetric with respect to inversion of the orientation of the initial $\vec{J}$ vector, which in Fig. 2.19 is parallel or anti-parallel to the Z-axis.

We now make use of the equal a priori probability of all angles ω to determine the probability of excitation to a certain level. Each energy level is artificially defined by a broad band. The separation between the levels is arbitrarily taken at half the energy distance between the levels. It can be shown that the final answer (the macroscopic measurable relaxation time) is not very much influenced by a shift of this boundary even to a quarter of the energy difference. Except for very low velocities, we found as a rule that the scattering angles for the trajectories, which resulted in a definite change of energy level, were grouped closely together around an average value. We used this average value $\overline{\chi}$ in the evaluation of the cross section. It may be remarked that this inelastic scattering angle associated with the process of excitation or de-excitation differs greatly in most cases from the scattering angle used in the previous section. There, we took the average over <u>all</u> phase angles ω, because both elastic and inelastic scattering phenomena were concerned. This time we use the fraction of all angles ω which gave rise to a definite transition from level i to j, as the probability f_{ij} of that particular transition. The differential excitation cross section σ_{ij} is then defined by

$$f_{ij}\,(b)\; b\; db \;=\; -\,\sigma_{ij}\,(\overline{\chi},\ \Theta_j,\ g)\quad \sin\overline{\chi}\; d\,\overline{\chi} \qquad (2.38)$$

In Fig. 2.20 the σ_{ij} are shown at $g^{*2} = 1$. In Fig. 2.21 the σ_{2j} are shown for $g^{*2} = 20$, as an example. The curves exhibit two kinds of maxima. All have local maxima at $\overline{\chi} = \pi$, corresponding to back scattering in the centre of mass system. This is a general property of inelastic scattering processes [33]). A second maximum occurs at lower scattering angles, sometimes so small that it only distorts the curve a little. This second maximum often exceeds the first, and is largest for the lowest quantum jumps $\Delta j = \pm 1$, where it is shifted to forward scattering, even to $\pi/4$. The curves are strongly energy dependent going through a maximum when the orbital and rotational angular momenta are of the same magnitude. Thereby the differential excitation and de-excitation cross

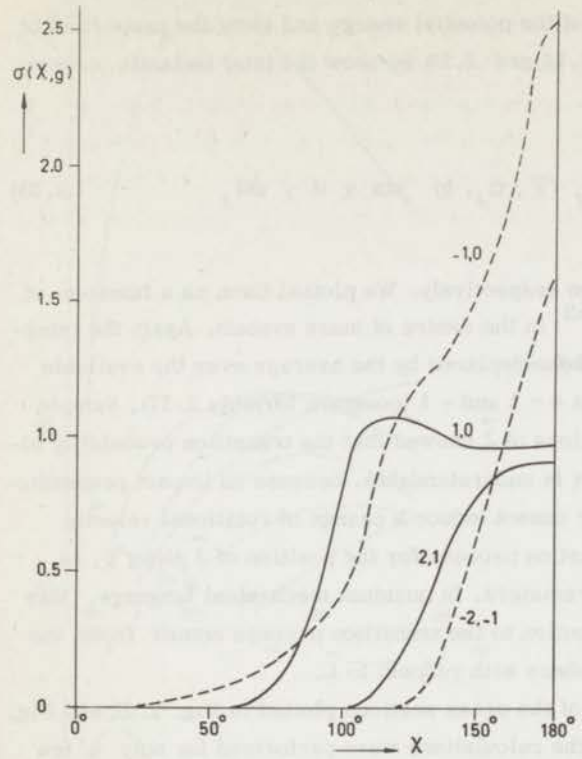

Fig. 2.20 Differential cross sections for rotational transitions at $g^{*2} = 1.021$ in the two-dimensional scattering system. The numbers indicate the transition from i → j.

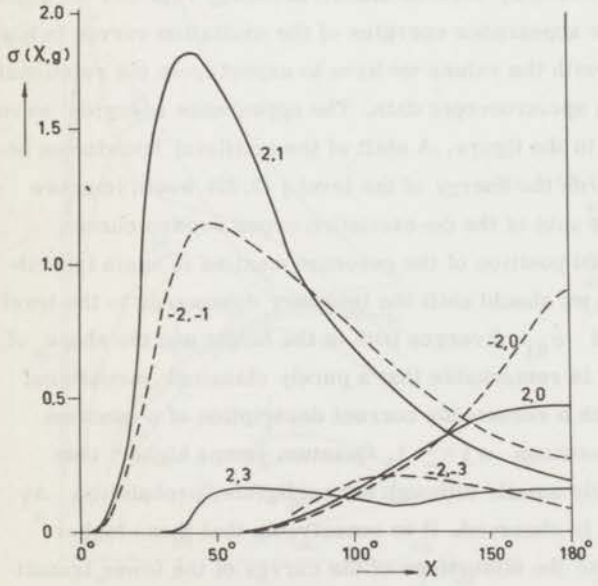

Fig. 2.21 See caption of Fig. 2.20. $g^{*2} = 20.417$.

sections follow the behaviour of the potential energy and show the properties of the rotating model. In Figs. 2.22 and 2.23 we show the total inelastic cross section

$$\sigma_{ij}\ (g^2) = -\int_0^{2\pi}\int_0^{\pi} \sigma_{ij}\ (\bar{\chi}, \Theta_J, g)\ \sin\chi\ d\chi\ d\Theta_J \qquad (2.39)$$

for excitation and de-excitation respectively. We plotted them as a function of the reduced relative energy g^{*2} in the centre of mass system. Again the integration over the angle Θ_J has been replaced by the average over the available orientations of the $\vec{J}$ vector, m = + 1 and - 1 (compare formula 2.37). Sample calculations for other orientations of $\vec{J}$ showed that the transition probability almost vanishes for m = 0. This is understandable, because an impact perpendicular to the plane of the rotator cannot induce a change of rotational velocity ($\vec{J}$ along X), whereas the excitation process for the position of $\vec{J}$ along Y, is limited to very low impact parameters. In quantum mechanical language, this implies that the major contribution to the transition process comes from the highest magnetic quantum numbers with respect to $\vec{L}$.

The numerical accuracy of the cross sections plotted in Fig. 2.22 and Fig. 2.23 is rather poor, because the calculations were performed for only a few impact parameters, widely spaced. Another, more fundamental error arises from the arbitrarily defined boundary between classical energy regions, to which a quantum was assigned. The appearance energies of the excitation curves in Fig. 2.22 do not coincide exactly with the values we have to expect from the rotational energy diagram, known from spectroscopic data. The appearance energies were indicated by vertical arrows in the figure. A shift of the artificial boundaries between the energy levels towards the energy of the level j (2.39) would improve the results. The same can be said of the de-excitation cross section curves (Fig. 2.23) where the expected position of the resonant maxima is again indicated by vertical arrows. Now, we should shift the boundary downwards to the level i. The behaviour of σ_{10} and σ_{01} diverges both in the height and the shape of the curves. Nevertheless, it is remarkable that a purely classical mechanical calculation could produce such a reasonably correct description of a quantum event, especially for the transitions $\Delta j = \pm 1$. Quantum jumps higher than $\Delta j = \pm 1$ have a comparatively small, although not negligible, probability. At high energies even $\Delta j = -4$ is observed. It is conceivable that these higher transitions are responsible for the distortions of the curves of the lower transit-

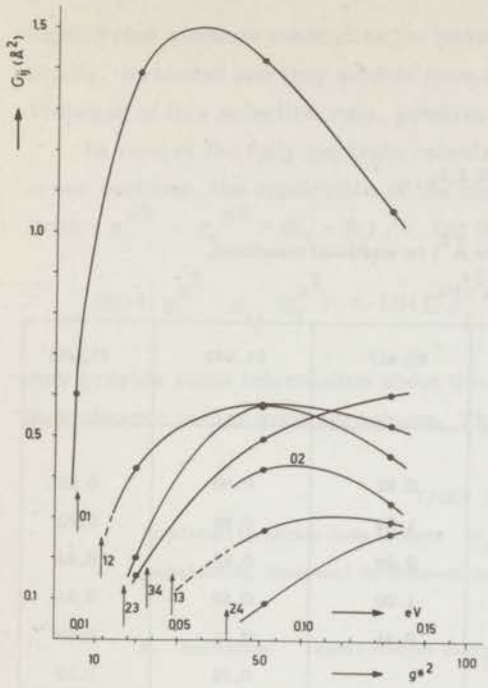

Fig. 2.22 Total cross sections for rotational excitation of HT in collisions with ^{4}He, as functions of energy, averaged over m = +1 and m = -1. The vertical arrows are the appearance energies expected from spectroscopical data. The 02-arrow is not shown.

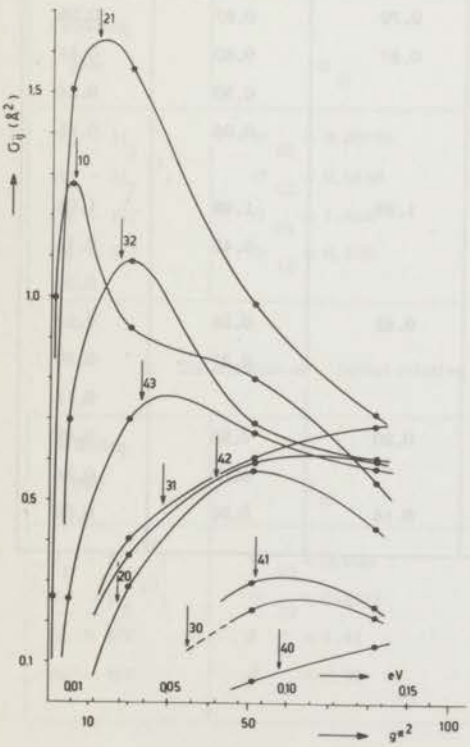

Fig. 2.23 Total cross sections for rotational deexcitation of HT in collisions with ^{4}He, as functions of energy, averaged over m = +1 and m = -1. The vertical arrows are the expected resonant energies.

TABEL 2.5.

Semi-classical cross sections σ_{ij} (in $\mathring{A}^2$) for rotational transitions, induced in HT by the collision with ^4He.

i → j \ g^{*2}	1.021	5.104	20.417	51.042	81.666
1 → 0	1.00	1.28	0.92	0.80	0.55
2 → 1	0.26	1.51	1.56	0.98	0.72
2 → 0			0.29	0.58	0.44
3 → 2		0.70	1.09	0.69	0.61
3 → 1			0.41	0.61	0.69
3 → 0				0.23	0.22
4 → 3		0.26	0.70	0.67	0.58
4 → 2			0.37	0.60	0.61
4 → 1				0.30	0.24
4 → 0				0.06	0.15
0 → 1		0.60	1.39	1.42	1.06
0 → 2				0.42	0.34
0 → 3					0.30
1 → 2			0.42	0.58	0.53
1 → 3				0.27	0.30
1 → 4					0.11
2 → 3			0.20	0.58	0.46
2 → 4				0.89	0.26
3 → 4			0.16	0.50	0.60

ions. From quantum mechanics we know that such transitions are, at least optically, forbidden and they seldom have been taken into account in calculations. Violation of this selection rule, however, can occur in collisional excitation.

In view of the fully separate calculations of the excitation and de-excitation cross sections, the application of the general relation between them [31] (with $g_j^{*2} - g_i^{*2} = (E_i - E_j)/\epsilon$ for the exchanged energy):

$$(2i+1)\, g_i^{*2}\ \sigma_{ij}\ (g_i^{*2}) = (2j+1)\, g_j^{*2}\ \sigma_{ji}\ (g_j^{*2}) \qquad (2.40)$$

may provide some information about the internal consistency of the results. We then observe rather good agreement. The compared values differ by a factor 2.

TABLE 2.6.

Rotational transition cross sections σ_{ij} (in Å^2) and transition probabilities, compared for different colliding molecules.

A. Excitation. Initial relative energy 0.05 eV.

Colliding pair	σ_{ij}	σ_{kin}	P_{ij}
$H_2 - H_2$ [33])	$\sigma_{02} = 0.00735$	20.6	$P_{02} = 0.00036$
$He - H_2$ [33])	$\sigma_{02} = 0.0148$	17.85	$P_{02} = 0.00081$
He - HT	$\sigma_{01} = 1.416$	17.35	$P_{01} = 0.0814$
He - HT	$\sigma_{12} = 0.335$	17.75	$P_{12} = 0.0188$

B. De-excitation. Initial relative energy 0.0259 eV.

Colliding pair	σ_{ij}	σ_{kin}	P_{ij}
$H_2 - H_2$ [33])	$\sigma_{20} = 0.020$	22.0	$P_{20} = 0.00091$
$He - H_2$ [33])	$\sigma_{20} = 0.2115$	19.0	$P_{20} = 0.0111$
He - HT	$\sigma_{21} = 1.41$	21.9	$P_{21} = 0.0645$
He - HT	$\sigma_{10} = 0.95$	19.5	$P_{10} = 0.0487$

It is not possible to compare our values with other theoretical or experimental results. In the literature, there is only a rather poor approximative treatment of the σ_{01} in HD by Takayanagi [31]), who obtained transition probabilities per collision larger than 1. From quantum mechanical theory Roberts [33]) computed transition cross sections for the collision of H_2 with He and with H_2. In Table 2.5 we compare his results with ours. We have also given a rough estimation of the transition probability per collision $P_{ij} = \sigma_{ij}/\sigma_{kin}$, where σ_{kin} is the elastic scattering cross section as it occurs in viscosity measurements. The large differences between the probabilities in He - H_2 and the H_2 - H_2 systems arise from the differences in the $V_2(r)$'s, which were employed by Roberts in the potentials underlying the calculations. A comparison with data from sound dispersion measurements [35]) shows that the theoretical values for H_2 - H_2 are wrong by a factor 3. The value of $V_2(r)$ is to be multiplied by 1.5 to obtain better agreement, which is not very pleasing because the potential was a theoretical one, derived from first principles [33]). The errors in our classical data being of the same order of magnitude as in the quantum mechanical case, we feel less reserved in exhibiting the results of our calculations.

2.7 CONCLUSIONS

The classical mechanical calculation of the orbit of a He atom colliding with a rigid rotator molecule HT, shows deviations from the scattering angle of the corresponding atom-atom collision, when the central symmetric potential is replaced by a potential which is still spherically symmetric about the geometrical midpoint of the molecule but which rotates together with the molecular axis around the centre of mass. The equations of motion exhibit separate terms for the contribution of centrifugal and Coriolis forces. The computer calculations of the cross sections derived from inelastic scattering show strong dependence on the initial orientation of the rotator axis and of the angular momentum, and on the relative angular momentum and energy of the particles.

An analysis of the effect of the space orientation of the angular momentum of the rotator shows a considerable polarization of the deviations of the cross sections. This point, as well as the effect of the collision on the position of the angular momentum, deserves further investigation in view of the anisotropy which they may introduce in the statistical distribution function. For the moment we took as an approximation to an orientation averaged cross section, the positions of $\vec{J}$ perpendicular to the collision plane as representative, which permitted a

simplification of the collision problem to only two-dimensional equations of motion.

Because of the long computing times the number of calculated orbits is only a test sample with respect to the required number for an accurate integration. The results, thus, show with a restricted accuracy that the transport cross sections for the different rotational states increase by some 20 %. The transition probabilities increase from 10^{-3} to about 5. 10^{-2}. These results are in qualitative agreement with the values which are to be expected from experiments. It is remarkable how correct a calculation based on classical mechanics can describe such a quantum phenomenon as the collision induced transition between rotational states.

CHAPTER 3

DIFFUSION AND THERMAL DIFFUSION IN GASEOUS MIXTURES WITH INTERNAL DEGREES OF FREEDOM

3.1 INTRODUCTION

There have been many excellent recent review articles on diffusion [1]) and thermal diffusion [2]) in gas mixtures with polyatomic components, in particular the hydrogen isotopes. We therefore feel that it is not necessary to give a general introduction to the subject. Thermal diffusion appears to be very sensitive to the characteristics of the collisions and the intermolecular potential. Apart from some subtile discrepancies [7]), the theory of Chapman and Enskog [8, 20]), using a spherically symmetric potential, succeeds very well in predicting the transport properties of symmetrical molecules. They behave approximately like atoms as we could confirm in Chapter 1.

The anomalous behaviour of a group of molecules with an asymmetric distribution of the atomic masses is therefore very interesting. The measured thermal diffusion factors depart so far from the calculated values [4,5]) and Chapter 1), that any improvement of the symmetrical potential theory fails to explain the discrepancy. On the other hand the special properties of the asymmetric molecules do not show up in the measured diffusion coefficients, which lie very close to those of the symmetric molecules [26, 40]). The introduction of assumptions about the perturbation of the symmetry and inelastic collision effects, unfortunately will lead to values of the diffusion coefficients departing very much from the experimental values. It was a challenge to many authors to find an answer to this problem and thus we could make use of several theoretical treatments available.

Wang Chang, Uhlenbeck and De Boer [9]) developed a formal kinetic theory for transport properties in gases, which includes the existence of internal degrees of freedom and inelastic collisions. Taxman [41]) did the same, but on a purely classical basis, considering the internal energy as a continuous quantity. New formulae were introduced for the collision integrals. A new characteristic time appeared connected with the relaxation of internal energy into translational energy. Monchick, Yun and Mason [10]) extended this theory to mixtures of gases. An attempt to evaluate the thermal diffusion factors was made by Monchick, Munn and Mason [42]). They expressed these factors as far as possible in terms of known experimental quantities, which were assumed to be insensitive to the potential model, but also used some data from theoretical calculations on atom-atom collisions. The calculations are based on the usual "semi-classical" assumption, which precludes any correlation between the internal state energy and the relative velocity (or scattering angle). The results are completely inadequate and, therefore, raise doubt about the validity of the expansion of the thermal diffusion factor into powers of the relaxation time, thereby assuming the inelastic terms in the collision integrals to be small. Waldmann [11]) and McCourt and Snider [12]) removed the restriction from the Wang Chang - Uhlenbeck theory, which consists in the fact that it does not account for the possible degeneracy of the internal states. This is the case for the rotational levels of hydrogen molecules, which we want to study in particular in view of our own experimental results. Although this improvement is of great theoretical significance, we have reasons to expect that the resulting corrections will not be of the required order of magnitude. They introduce merely second order effects on the transport properties due to angular momentum anisotropy.

From quite another point of view, systems with internal degrees of freedom can be treated with thermodynamics of irreversible processes (Ref. 43, p. 221). This may be done by the introduction of a continuous internal configuration space [44]) (in analogy with the classical model of Taxman). It may also be applied by considering the internal quantum states as separate components of a chemically reacting mixture [43]) (which corresponds more to the Wang Chang - Uhlenbeck treatment). Meixner [45]) proved the great value of this kind of approach, by deriving macroscopic expressions for the heat conductivity of gases with rotational states, which account for the deviations introduced by the influence of additional heat transfer and transitions between quantum states. We intend to show that the chemical reaction concept introduces an additional mass and heat transfer mechanism in diffusion and thermal diffusion of hydrogen.

The influence of chemical reactions on the distribution of the components of a mixture in a temperature gradient has been described a long time ago [46, 47]. At least this influence is of the first order.

3.2 THE DIFFUSION COEFFICIENT

Let us consider a mixture of two gases, α and β, one of which, say β, consists of atoms with a spherically symmetric interaction potential, for instance an inert gas. The first component, α, consists of diatomic molecules with internal degrees of freedom, which may be rotational or vibrational states. Such a molecule, when colliding with an inert gas atom, does not have a spherically symmetric potential, but as long as it is homonuclear, this is a good approximation. For heteronuclear molecules, however, the centre of the potential rotates around the centre of mass of the molecule, or vibrates about the equilibrium position, which is no longer the geometrical midpoint of the molecule. As was shown in the preceding paper, considerable deviations follow for the scattering and rotational excitation cross sections. These deviations depend strongly on the quantum number involved. For these molecules, where the different scattering for each of the internal states becomes of importance, a modification is required of the equations underlying the calculation of the transport coefficients. The new feature is conveniently described in terms of chemical reactions, which can be said to occur between the internal states, under the influence of collisions:

$$\alpha_1 \rightleftharpoons \alpha_2, \quad \alpha_1 \rightleftharpoons \alpha_3, \quad \text{etc.}$$

In these reactions translational energy of the particles is transformed into internal heat. The reaction also changes the identity of the particle. On the other hand the identity of the particles does not appear in the macroscopic measurement, where only the concentration of α as a whole is measured. The formalism for the latter aspect of the measurement, was developed by Prigogine and Buess [46] to calculate thermal diffusion coefficients in mixtures where a true chemical reaction was involved. Their case was the particular case of chemical equilibrium, i.e. very high reaction velocity. Now, the hydrodynamic relaxation times involved in transport properties are mostly large with respect to the relaxation times which occur in the establishment of the stationary state of an equilibrium distribution between the internal degrees of freedom. Thus, the chemical equilibrium is not a bad assumption. If, however, the reactions are

very slow, the treatment can be refined according to De Groot and Mazur [43], who conserved the dependency of the phenomenon on the reaction velocity.

The phenomenological equation for the diffusion flow of component α in a binary mixture with β, reads

$$\vec{J}_\alpha = - \rho \mathcal{D} \operatorname{grad} n_\alpha , \tag{3.1}$$

where $\vec{J}_\alpha$ is the mass flux of component α, defined by

$$\vec{J}_\alpha = \rho c_\alpha (\vec{v}_\alpha - \vec{v}), \tag{3.2}$$

TABLE 3.1

Notation

ρ_i = mass density of the i'th component ; $\sum_{i=1}^{n} \rho_i = \rho$;

ρ = total mass density of the mixture ;

$c_i = \rho_i/\rho$ = mass fraction ; $\sum_{i=1}^{n} c_i = 1$;

N_i = molar density of the i'th component; $\sum_{i=1}^{n} N_i = N$;

N = total molar density.

$n_i = N_i/N$ = molar fraction or concentration ; $\sum_{i=1}^{n} n_i = 1$;

$\rho_i = M_i N_i$; M_i = molar weight of the i'th component ;

M = reduced mass of the colliding particles ;

κ = Boltzmann's constant.

Here $\vec{v}$ is the centre of mass velocity of the mixture and $\vec{v}_\alpha$ is the flow velocity of component α. From (3.2) we have

$$\vec{J}_\alpha = - \vec{J}_\beta \, . \tag{3.3}$$

The coefficient $\mathcal{D}$ is the measurable binary diffusion coefficient. The other symbols are defined in Table 3.1. Let the component α consist of a finite set $j = 1, \ldots, n-1$ of internal states. Then, the measured grad n_α equals

$$\text{grad } n_\alpha = \text{grad } \left(\sum_{j=1}^{n-1} n_j \right), \tag{3.4}$$

Let the component β be the n'th component,

$$\text{grad } n_\beta = \text{grad } n_n \, .$$

The mixture is now to be considered as a multicomponent mixture of n components, and the diffusion equation becomes

$$\vec{J}_\beta = \vec{J}_n = - \rho \, c_n \sum_{j=1}^{n-1} (D_{nj} - D_{nn}) \text{ grad } n_j, \tag{3.5}$$

where the D_{ik} are the multicomponent diffusion coefficients (Waldmann [14]).

Let us now assume local chemical equilibrium between all pairs of components of α. The chemical equilibrium condition for unimolecular reactions, $\alpha_i \rightleftharpoons \alpha_k$, is given by

$$\mu_i = \mu_k \tag{3.6}$$

where μ_i are the thermodynamic potentials of the components, i, k = 1, ... n - 1. Now, for ideal mixtures, we have by definition,

$$\mu_i = \frac{RT}{M_i} \ln n_i + C_i \, (T), \tag{3.7}$$

where R is the gas constant, and C depends only on the temperature. Taking the gradient of equation (3.6) at constant temperature and pressure, we obtain (n - 1) (n - 2) / 2 relations between the n - 1 components of α in the mixture:

$$c_k \text{ grad } n_i = c_i \text{ grad } n_k \, ; \, (i \neq k). \tag{3.8}$$

This relation is equivalent to the statement that the local equilibrium distribution of the components of α is conserved, independent of the gradient in the total concentration of α. On purpose we wrote Eq. (3.8) in the present form, using the unimolecular character of the reaction, $M_i = M_k$, because the summational relations apply :

$$\sum_{l=1}^{n} c_l D_{il} = 0. \tag{3.9}$$

We then get from (3.5), for every i

$$\vec{J}_n = \rho \frac{c_n}{c_i} D_{nn} \text{ grad } n_i, \tag{3.10}$$

or, summing over all components,

$$\text{grad} \left(\sum_{i=1}^{n-1} n_i \right) = \frac{1 - c_n}{\rho c_n D_{nn}} \vec{J}_n \tag{3.11}$$

The expression for the measured diffusion coefficient $\mathcal{D}$ is obtained from a comparison between (3.1) and (3.11), using (3.3)

$$\mathcal{D} = \frac{c_n}{1 - c_n} D_{nn} \tag{3.12}$$

In order to be accessible to calculations the multicomponent diffusion coefficient D_{nn} has to be expressed in terms of the cross sections for the binary collisions between atoms and molecules in different internal states. To this end a solution is required of the Boltzmann equation [8,14,20]), which describes the microscopic space-time behaviour of the singlet distribution function $f_i(\vec{u}_i; \vec{r}, t)$, where $\vec{u}_i$ is the velocity of the particles of state i. A modification of the Boltzmann equation given by Wang Chang, Uhlenbeck and De Boer [9]), takes into account the existence of internal degrees of freedom and transitions between them. This treatment, which pertained to a single gas component, has to be extended to mixtures. Monchick, Yun and Mason [10]) and Waldmann and Trübenbacher [48]) performed a formal extension of this kind. We note that in these extensions as well as in the main body of ref. 9, the transition rate between translational and internal degrees of freedom is supposed to be high. This is why these formalisms are all based on a zero order Maxwell distribution function $f_i^{(o)}$, multiplied by a Boltzmann distribution over the internal states based on the same

temperature T. This implies that the state of the gas can be described by only one temperature for both translational and internal degrees of freedom.

Now, from a comparison of the treatment of Waldmann and Trübenbacher [48]) with the older simple solution of the Boltzmann equation in the case of atomic collisions [14]), it can be seen that the transformation of the multicomponent diffusion coefficients in terms of the development coefficients $\vec{A}$ of the diffusion part of the Chapman - Enskog perturbation function $\phi_i^{(1)}$, or in terms of the binary diffusion coefficients between the components remains of the same mathematical form, wether there are transitions or not. The development coefficients describe vectorial phenomena and thereby cannot depend explicitly on the scalar rates of transition. So far we can proceed with our theory. Next, these coefficients have to be expressed in terms of new collision integrals [10]) which contain the inelastic cross sections for diffusional phenomena.

However, these treatments are inconsistent with the fundamental requirements of our phenomenological theory which stems on thermodynamics of irreversible processes. We considered every internal state to be a separate entity, reaching the local Maxwell distribution within microscopic times (10^{-8} sec.) which are short with respect to the establishment of equilibrium between internal states (10^{-6} sec.). The reaction rate still can be said to be infinite from the macroscopic point of view, where the hydrodynamic relaxation times are of importance ($> 10^{-2}$ sec.). The number of collisions involved in rotational transitions with hydrogen isotopes fits into this scheme. The exchange of energy and the existence of a different internal temperature have already been accounted for in our treatment by the use of the concept of chemically reacting components. Therefore, we stay with the solution of the Boltzmann equation in the early fashion [14, 20]) and the simple collision integrals developed in this treatment. A kinetic theory which would parallel our treatment, has to be developed along the line of a "slow, but not negligible exchange"- case (App. ref. 9), which discerns between a translational temperature and an internal temperature. The expressions for the transport coefficients would still contain terms depending on a finite transition rate or relaxation time.

There is an objection against the use of the multicomponent theory of Hirschfelder, Curtiss and Bird [20]). Their definition of the transport coefficients cannot be used for extension to systems with reaction between the different species [49]). If such systems are to be treated with the formalism of thermodynamics of irreversible processes, full symmetry of the coefficients is required in the sense of Onsager's relations. Following the treatment of Waldmann [14]) which

meets this requirement, we have

$$D_{nn} = \sum_{l,j}^{n} \frac{c_l\, c_j}{2\,\nu} \left\{ A^{(n)}_{n,0} - A^{(n)}_{l,0} - A^{(j)}_{n,0} + A^{(j)}_{l,0} \right\} \tag{3.13}$$

where $A^{(k)}_{i,0}$ are the coefficients of the development in Sonine polynomials of the diffusion term in the Chapman - Enskog distribution function. ν is the total particle number density. The coefficients A may be expressed as a function of the collision integrals Ω, by obtaining them from the relations (in Waldmann's approximation) :

$$\sum_{j=1}^{n} \frac{16\ \rho^2\, \Omega^{(1,1)}_{ij}\ c_i c_j\ (A^{(k)}_{i,0} - A^{(k)}_{j,0})}{6\ N\ \kappa\ T\ (M_i + M_j)\ \nu} = \delta_{ik} - n_i\ ; \tag{3.14}$$

$$(i,\ k = 1,\ \ldots.,\ n).$$

Because the set of equations (3.14) is not independent, one has to take into account

$$\sum_{j=1}^{n} c_j\ A^{(k)}_{j,0} = 0. \tag{3.15}$$

Fortunately, the set of equations (3.14) and (3.15) breaks down into n different sets for each i. Each has the same Cramer-determinant, the elements of which are :

$$\begin{aligned} a_{ii} &= \sum_{k=1}^{n} c_k\ (1 - \delta_{ik})\ \Omega^{(1,1)}_{ik} / (M_i + M_k), \\ a_{ij} &= -\ c_i\ \Omega^{(1,1)}_{ij} / (M_i + M_j) \\ a_{in} &= 0, \qquad a_{nj} = c_j, \qquad a_{nn} = 1, \end{aligned} \tag{3.16}$$

leaving out the constants.

For example, for n = 3 (i.e. two internal states of the α particles) equation (3.13) then becomes

$$D_{33} = \frac{3N\kappa T}{16\ \rho^2} \frac{\frac{(c_1+c_2)^2}{c_3}\ \Omega_{12}^{(1,1)\ddagger} + c_1\,\Omega_{23}^{(1,1)\ddagger} + c_2\Omega_{13}^{(1,1)\ddagger}}{c_1\Omega_{12}^{(1,1)\ddagger}\ \Omega_{13}^{(1,1)\ddagger} + c_2\Omega_{12}^{(1,1)\ddagger}\ \Omega_{23}^{(1,1)\ddagger} + c_3\,\Omega_{13}^{(1,1)\ddagger}\Omega_{23}^{(1,1)\ddagger}} \qquad (3.17)$$

where, for brevity $\Omega_{ij}^{(1,1)\ddagger}$ stand for $\Omega_{ij}^{(1,1)} / (M_i + M_j)$.

The generalization to more internal states is straightforward.

In view of the application we want to make in section 4 of this chapter, we also require the component α to be in trace concentration:

$$N_j \ll N_\beta \simeq N .$$

Then, using again the equality of the molecular masses,

$$M_j = M_\alpha ; \qquad j = 1, \ldots\ldots, n-1 ;$$

equation (3.12) becomes

$$\mathcal{D} = \frac{3N\kappa T}{16\ \rho^2} (M_\alpha + M_\beta) \sum_{j=1}^{n-1} \frac{\gamma_j}{\Omega_{jn}^{(1,1)}} , \qquad (3.18)$$

where the γ_j are the normalized occupation numbers for the internal states:

$$\gamma_j = N_j \Big/ \sum_{k=1}^{n-1} N_k . \qquad (3.19)$$

As Ω_{jn} we take the usual collision integrals defined by Waldmann [14], but now every internal state has its own Ω_{jn}. The transport cross sections for nearly elastic scattering on which these Ω - integrals are based were defined and calculated in section 2.5. Because of the necessity of maintaining the effect of inelastic collisions on the scattering, we integrated the differential cross sections over all scattering angles including those arising from inelastic collisions. Also we took into account various differences in relative velocity before and after the collision. The number of collisions which deserve to be called inelastic in the quantum mechanical sense is small, so that the cross sections will be close to the elastic limit. The cross sections being averaged

over all space orientations of $\vec{J}$ fulfil the symmetry relations with respect to space and time inversion, such as are required in the solution of the Boltzmann equation [48]).

3.3 THE THERMAL DIFFUSION FACTOR [50])

A treatment similar to that of the preceding section can be given if the system is subjected to a temperature gradient. Equation (3.5) is replaced by

$$\vec{J}_\beta = \vec{J}_n = \rho \sum_{j=1}^{n-1} c_j D_j \frac{T \operatorname{grad} T}{T} - \rho c_n \sum_{j=1}^{n-1} (D_{nj} - D_{nn}) \operatorname{grad} n_j, \qquad (3.20)$$

where the D_j^T are the thermal diffusion coefficients of a multicomponent mixture. Equilibrium between the internal degrees of freedom is again assumed and from (3.6) we obtain

$$\left(\frac{\partial \mu_i}{\partial n_i}\right)_{p,T} \operatorname{grad} n_i + \left(\frac{\partial \mu_i}{\partial T}\right)_{n_i,p} \operatorname{grad} T = \left(\frac{\partial \mu_k}{\partial n_k}\right)_{p,T} \operatorname{grad} n_k + \left(\frac{\partial \mu_k}{\partial T}\right)_{n_k,p} \operatorname{grad} T. \qquad (3.21)$$

The (n-1)(n-2) / 2 auxiliary relations now are

$$\operatorname{grad} n_i = \frac{n_i M_i}{n_k M_k} \operatorname{grad} n_k + \frac{n_i M_i}{RT^2} (h_i - h_k) \operatorname{grad} T, \qquad (3.22)$$

where h_i is the enthalpy per unit mass of the i'th component. $(h_i - h_k)$, consequently, is the difference in heat content between the two internal states i and k. In other words, it is the translational energy, which may be set free in the de-excitation reaction.

The stationary state reached by the thermal diffusion process is now not necessarily characterized by

$$\vec{J}_i = 0,$$

because, due to the switch in identity of the particles in the chemical reaction, it is possible that they move as component i in the direction of the temperature gradient and come back as k. The stationary state is, however, still adequately

described by the condition that the mass flow of the inert component vanishes,

$$\vec{J}_n = 0. \tag{3.23}$$

From (3.20), (3.22) and (3.23) we obtain, using $\sum_{j=1}^{n} c_j D_j^T = 0$,

$$D_n^T \frac{\operatorname{grad} T}{T} = - \sum_{k=1}^{n-1} (D_{kn} - D_{nn}) \frac{n_k M_k}{n_i M_i} \operatorname{grad} n_i - \sum_{k=1}^{n-1} (D_{kn} - D_{nn}) \frac{n_k M_k}{RT^2} (h_k - h_i) \operatorname{grad} T, \tag{3.24}$$

and

$$\frac{\operatorname{grad} n_i}{n_i M_i} = \frac{D_n^T \frac{\operatorname{grad} T}{T} + \sum_{k=1}^{n-1} (D_{kn} - D_{nn}) \frac{n_k M_k}{RT^2} (h_k - h_i) \operatorname{grad} T}{- \sum_{k=1}^{n-1} (D_{kn} - D_{nn}) n_k M_k} \tag{3.25}$$

With help of the definitions of Table 3.1 and the relation

$$\sum_{j=1}^{n} c_j D_{jk} = 0, \tag{3.9}$$

this may be simplified to

$$\operatorname{grad} n_i = \frac{c_i D_n^T + \sum_{k=1}^{n-1} (D_{kn} - D_{nn}) \frac{\rho}{NRT} c_k c_i (h_k - h_i)}{D_{nn}} \frac{\operatorname{grad} T}{T}. \tag{3.26}$$

Applying again the principle of formula (3.4), we obtain

$$\sum_{i=1}^{n-1} \operatorname{grad} n_i = \operatorname{grad} n_\alpha = \left[\frac{(1-c_n) D_n^T}{D_{nn}} - \frac{\rho}{NRT} \sum_{k>i}^{n-1} \frac{D_{kn} - D_{in}}{D_{nn}} \times c_k c_i (h_k - h_i) \right] \frac{\operatorname{grad} T}{T} \tag{3.27}$$

We now introduce the same simplifications which led to equation (3.18) in the case of diffusion. Thus, for trace concentration of α in β

$$\alpha_\infty = - \frac{T \operatorname{grad} n_\alpha}{n_\alpha n_\beta \operatorname{grad} T} = \alpha_{bin} - \frac{N M_\alpha M_\beta}{\rho RT} \sum_{k>i}^{n-1} \left\{ \frac{\frac{1}{\Omega^{(1,1)}_{kn}} - \frac{1}{\Omega^{(1,1)}_{in}}}{\frac{1}{\gamma_k \Omega^{(1,1)}_{in}} + \frac{1}{\gamma_i \Omega^{(1,1)}_{kn}}} \right\} (h_k - h_i), \tag{3.28}$$

where α_∞ and α_{bin} are the thermal diffusion factors at chemical equilibrium and for the equivalent binary mixture of atoms, respectively. The identification of α_{bin} with

$$\alpha_{bin} = \frac{(1 - c_n) D^T_n}{D_{nn}}, \tag{3.29}$$

is justified only when D_{nn} does not differ much from the binary coefficient, occurring when no reaction takes place. Then

$$\operatorname{grad} n_\alpha = - \alpha_{bin} n_\beta n_\alpha \frac{\operatorname{grad} T}{T} = - \frac{D^T_\alpha}{D_{\alpha\alpha} - D_{\beta\beta}} \frac{\operatorname{grad} T}{T}$$

$$= \frac{c_\alpha D^T_\beta}{D_{\beta\beta}} \frac{\operatorname{grad} T}{T} . \tag{3.30}$$

3.4 COLLISION INTEGRALS AND CALCULATION OF THE COEFFICIENTS

The calculation of the collision integrals $\Omega^{(\ell, s)}$ is accomplished by means of the well known formula [20])

$$\Omega^{(\ell,s)^*}_{jn} = \frac{2}{(s+1)\,!\; T^{*\,s+2}} \int_0^\infty e^{-g^{*2}/T^*} g^{*\,2s+3} Q^{(\ell)^*}_{jn} dg^*, \tag{3.31}$$

where $g^{*2} = M g^2/2\varepsilon$ is the reduced relative kinetic energy and $T^* = \kappa T/\varepsilon$ is the reduced temperature. We prefer to work with quantities T^* and g^*, reduced with respect to the depth ε of the potential well, because most numerical tables make use of these units. Using the combining rules for ε, the transport coefficients for every pair of atoms can be calculated from the reduced $\Omega^*(T^*)$. However, in the case of molecules with internal degrees of freedom, this advantage is lost because each internal quantum state j has a characteristic ro-

tational energy and a characteristic rotational temperature. This makes it impossible to generalize the calculation of the scattering cross section of section 2.5 so as to find the values for other molecules from the calculation of one "reduced" molecule. For convenience the collision integrals are divided by their rigid sphere values (indicated by *), as was done by Hirschfelder, Curtiss and Bird [20]. From the scattering cross sections $Q_{jn}^{(\ell)*}$, which were calculated with the rotating potential model in section 2.5, we evaluated the collision integrals $\Omega_{jn}^{(\ell,s)*}$ of equation (3.31). The results are shown in Tables 3.2, 3.3 and 3.4. In Fig. 3.1 and 3.2 the deviations are shown between the former collision integrals and the $\Omega_{\alpha\beta}^{(\ell,s)*}$ values for a spherically symmetric potential model (compare Ref. 20, p. 1126). The latter are also given, in the first rows

TABLE 3.2

Collision integrals for the diffusion of the rotational states of HT in ^{4}He.

T^*	$\Omega_{\alpha\beta}^{(1,1)*}$	$\Omega_{0n}^{(1,1)*}$	$\Omega_{1n}^{(1,1)*}$	$\Omega_{2n}^{(1,1)*}$	$\Omega_{3n}^{(1,1)*}$	$\Omega_{4n}^{(1,1)*}$
3	0.9490	0.842	1.053	1.314	1.402	1.322
4	0.8836	0.781	0.941	1.163	1.264	1.259
5	0.8422	0.7464	0.8752	1.0680	1.1761	1.2101
8	0.7712	0.6981	0.7790	0.9189	1.0270	1.1077
10	0.7424	0.6825	0.7469	0.8662	0.9669	1.0567
20	0.6640	0.6363	0.6690	0.7363	0.8035	0.8833
30	0.6232	0.6048	0.6270	0.6706	0.7187	0.7786
50	0.5756	0.5651	0.5771	0.5983	0.6249	0.6589
80	0.5352	0.530	0.535	0.545	0.557	0.573

TABLE 3.3

Collision integrals for the thermal diffusion of the rotational states of HT in ^{4}He.

T^*	$\Omega_{\alpha\beta}^{(1,2)*}$	$\Omega_{0n}^{(1,2)*}$	$\Omega_{1n}^{(1,2)*}$	$\Omega_{2n}^{(1,2)*}$	$\Omega_{3n}^{(1,2)*}$	$\Omega_{4n}^{(1,2)*}$
3	0.8640	0.708	0.922	1.247	1.402	1.441
4	0.8167	0.675	0.837	1.103	1.274	1.370
5	0.7847	0.6590	0.7895	1.0157	1.1901	1.3143
8	0.7260	0.645	0.7257	0.8863	1.0364	1.1864
10	0.7013	0.6409	0.7048	0.8399	0.9706	1.1178
20	0.6293	0.6028	0.6367	0.7055	0.7819	0.8802
30	0.5909	0.5723	0.5943	0.6334	0.6828	0.7465
50	0.5459	0.5369	0.5463	0.5609	0.5821	0.6103
80	0.5075	0.504	0.507	0.512	0.519	0.529

TABLE 3.4

Collision integrals for the viscosity of the rotational states of HT in ^{4}He.

T^*	$\Omega^{(2,2)*}_{\alpha\beta}$	$\Omega^{(2,2)*}_{0n}$	$\Omega^{(2,2)*}_{1n}$	$\Omega^{(2,2)*}_{2n}$	$\Omega^{(2,2)*}_{3n}$	$\Omega^{(2,2)*}_{4n}$
3	1.0390	1.074	0.906	0.581	0.426	0.512
4	0.9700	1.002	0.897	0.669	0.515	0.497
5	0.9269	0.9604	0.8892	0.7129	0.5724	0.5018
8	0.8538	0.8991	0.8729	0.7597	0.6625	0.5442
10	0.8242	0.8759	0.8619	0.7681	0.6901	0.5716
20	0.7432	0.8043	0.8011	0.7575	0.7212	0.6423
30	0.7005	0.7576	0.7533	0.7297	0.7066	0.6571
50	0.6502	0.6865	0.6832	0.6736	0.6622	0.6412
80	0.5973	0.613	0.611	0.608	0.603	0.596

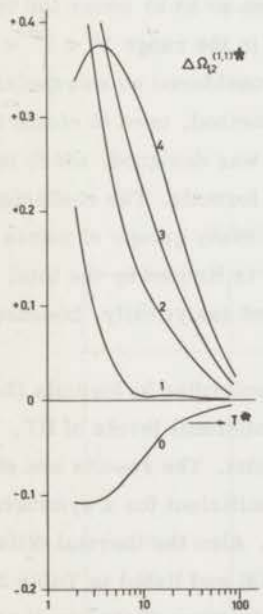

Fig. 3.1 Correction on the collision integral $\Omega^{(1,1)*}_{HT,He}$ for different rotational states of HT.

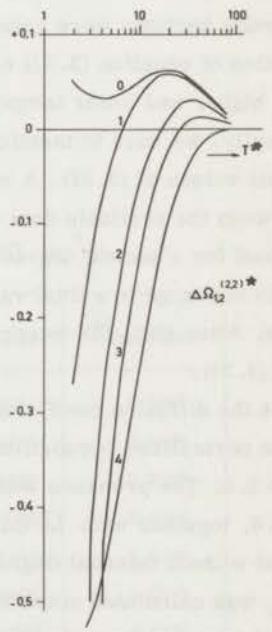

Fig. 3.2 Correction on the collision integral $\Omega^{(2,2)*}_{HT,He}$ for different rotational states of HT.

of Tables 3.2, 3.3 and 3.4. The Lennard - Jones 12-6 potential has been used throughout this paper. There are some comments to be made with respect to the accuracy of the new collision integrals. We wanted to have scattering cross sections, averaged over all magnetic substates of the rotational levels. This implied averaging over all possible orientations in space of the rotational vector $\vec{J}$ in the HT molecule. It was impossible to fulfil this requirement because of the computing time, which would have become excessive. We confined the calculations to m = + 1 and - 1 with respect to the orbital angular momentum $\vec{L}$ of the colliding atom (Section 2.5). Test samples of other orientations of $\vec{J}$ showed that this is not a bad approximation. The second restriction pertains to the fact that the calculations of section 2.5 were performed on the basis of classical mechanics. The results, therefore, suffer from the approximate character of classical mechanics at low velocities and small impact parameters. With light molecules, such as helium and hydrogen, quantum mechanical corrections start to be important at $T^* < 5$ [27]. On the other hand, the velocities g^* for which the scattering cross sections were calculated, were chosen so as to cover the velocity distribution of equation (3.31) as well as possible in the range $10 < T^* < 30$. The data for higher and lower temperatures must be considered as extrapolations.

Finally, we have to mention the integration method, used to obtain the numerical values of (3.31). A machine procedure was designed, which interpolated between the available data with the Lagrange formula. The coefficients were determined for a second degree curve through as many groups of points as were needed to converge to a final value. The accuracy is limited by the total number of points. After that, the integral could be obtained analytically, because of the form of (3.31).

Then the diffusion coefficient was calculated according to formula (3.18), using the normalized occupation numbers of the rotational levels of HT, shown in Table 3.5. The pressure was assumed to be 1 atm. The results are shown in Table 3.6, together with $\mathcal{D}(\alpha, \beta)$, the diffusion coefficient for a symmetric potential model without internal degrees of freedom [20]. Also the thermal diffusion factor α_∞ was calculated according to formula (3.28) and listed in Table 3.7. We neglected quantum jumps larger than $\Delta j = \pm 1$, because of the small probability of such transitions. The assumption of chemical equilibrium would break down. The first row of Table 3.7 again gives the value of α_{bin} for a symmetric potential and without internal states (section 1.4).

TABLE 3.5.

Normalized occupation numbers of the rotational levels of HT.

T^*	Y_0	Y_1	Y_2	Y_3	Y_4
3	0.7053	0.2859	0.0087	0	0
4	0.5798	0.3877	0.0321	0.0005	0
5	0.4892	0.4416	0.0667	0.0025	0
8	0.3306	0.4682	0.1739	0.0256	0.0016
10	0.2714	0.4467	0.2240	0.0518	0.0060
20	0.1459	0.3241	0.2963	0.1685	0.0652
30	0.1050	0.2579	0.2881	0.2212	0.1277
50	0.0754	0.2006	0.2630	0.2568	0.2042
80	0.0607	0.1688	0.2421	0.2707	0.2577

TABLE 3.6.

Diffusion coefficient of trace HT in ^{4}He.

T^*	$\mathcal{D}_{(\alpha,\beta)}$	$\mathcal{D}_{\text{Mason}}$	$\mathcal{D}_{\text{this paper}}$
3	0.0815	0.0757	0.0863
4	0.1348	0.1253	0.1408
5	0.1976	0.1826	0.2038
8	0.4367	0.3935	0.4346
10	0.6340	0.5643	0.6184
20	2.0048	1.7405	1.8632
30	3.9243	3.3763	3.6352
50	9.1276	7.8774	8.6242
80	19.883	17.606	19.261

TABLE 3.7.

Thermal diffusion factor of trace HT in ^{4}He.

T^*	α_{bin}	α_{Mason}	$\alpha_{this\ paper}$
3	0.0262	0.0065	- 0.0673
4	0.0286	0.0129	- 0.0525
5	0.0296	0.0181	- 0.0411
8	0.0294	0.0292	- 0.0227
10	0.0309	0.0357	- 0.0133
20	0.0317	0.0408	+ 0.0077
30	0.0318	0.0377	+ 0.0172
50	0.0318	0.0322	+ 0.0257
80	0.0280	0.0265	+ 0.0259

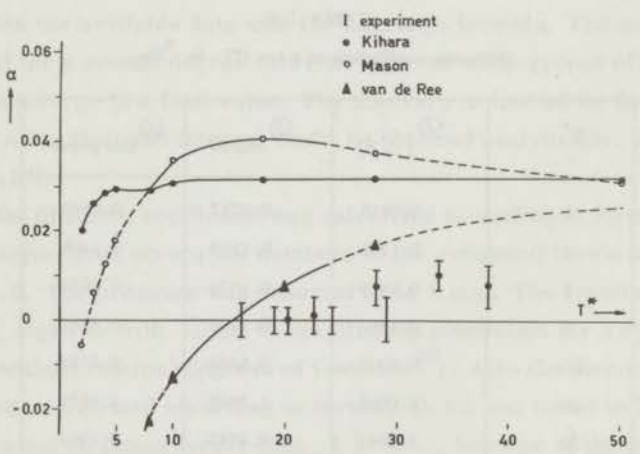

Fig. 3.3 Thermal diffusion factor for HT - ^{4}He.

Note added in proof: Recently, the experimental value $\alpha = 0.001$ was found by us, at $T^* = 10$.

3.5 DISCUSSION OF THE THEORETICAL RESULTS AND COMPARISON WITH EXPERIMENT

So far as the diffusion coefficient is concerned, no asymmetry effect could be detected experimentally. Both groups of experiments, the older ones of Mason , discussed again in a paper by Mason, Amdur and Oppenheim [1], and the more recent work of Reichenbacher, Müller and Klemm [26], give relative values of the quantities $\sqrt{M}\,\mathcal{D}$ for symmetric and asymmetric hydrogen isotopes, very close to 1. The fact that our theoretical values, in spite of our more complete treatment, stay so close to the older values $\mathcal{D}(\alpha, \beta)$, is a remarkably negative confirmation of the theory. It is due to the compensation of the negative deviations of the omega integrals of the lower quantum states, by the positive deviations of the higher quantum numbers. The population of these levels is determined by the temperature distribution function. On the other hand, the thermal diffusion factors are in good agreement with the experimental values measured by ourselves (Fig. 3.3) and with the experiments of Reichenbacher and Klemm [4], where the second partner is a spherically symmetric D_2 molecule. At high temperatures the agreement is not so good, but we must remark that, as can be seen from Table 3.5, the effect of the quantum numbers higher than 4 is very large in this region. The positive deviations in $\Omega^{(1,1)}$ for $j = 5$ or 6 are still higher than those for $j = 4$. The resulting correction on the thermal diffusion factor will lower the theoretical curve in the high temperature region. The statement of equation (3.29) may now be justified, as the quantity D_{nn} appears to differ so little from the value for a binary mixture which does not have the complication of internal degrees of freedom and asymmetric mass distribution in the molecules. If this assumption was not valid, this part of formula (3.28) should have been calculated separately, using the new values of the collision integrals.

At this point of the discussion a serious objection rises against using an $\Omega^{(\ell,s)}_{\alpha\beta}$ averaged over all rotational states, as suggested by Monchick, Yun and Mason [10]. The averaging procedure

$$\Omega^{(\ell,s)}_{\alpha\beta} \equiv \Omega^{(\ell,s)}_{qq'} = \left[\sum_i \exp(-\epsilon_{qi})\right]^{-1} \sum_i \exp(-\epsilon_{qi})\, \Omega^{(\ell,s)}_{qi,q'}$$

$$\equiv \sum_i \gamma_i \Omega^{(\ell,s)}_{in} \qquad (3.32)$$

is a simple arithmetic mean which applies only in the limiting case that the inter-

change of translational and rotational energy is very easy on the microscopic scale, that is when the energy distribution can be defined by only one temperature (Section 3.2). In this case the effect of a difference between the kinetic and the rotational relaxation times is blurred. The calculation of the diffusion coefficient or the thermal diffusion factor of HT - ^{4}He with formula (3.32), inserted in the expressions given by the same authors, give erroneous results even when the new collision integrals of Tables 3.2, 3.3 and 3.4 are used. The diffusion coefficients obtained in this way depart from the experimental value by a considerable amount. The thermal diffusion factor is only influenced by a small deviation, which furthermore, is in the wrong direction (Tables 3.6 and 3.7, Fig. 3.3). In a more recent paper, Monchick, Munn and Mason [42]) derived correction terms for the effect of inelastic collisions by introducing relaxation times and energy exchange corrections into their previously derived relations. The thermal diffusion factor of the D_2 - HT mixture was only improved by 0.00018. From the possible reasons for the failure of the theory, indicated by these authors, we now believe on basis of our calculations, that for asymmetric molecules, the intermolecular potential is indeed strongly dependent on the orientation. The result of this is the combined effect of the inelasticity of the collision and the correlated deviation of the scattering angle (section 2.5). There have been calculations of cross sections with simplified models, rough spheres, spherocylinders and loaded spheres [51]). The last one is perhaps closest to the model we chose, which we wanted to be as realistic as possible. However, these models were only applied to the evaluation of heat conductivity and viscosity in pure gases. On basis of the loaded sphere model Sandler and Dahler [53]) calculated in a recent paper the thermal diffusion factor for D_2 - HT, a system which has a close analogy to He - HT. For the first time a reasonable value was obtained, 0.052 (neglecting the contribution of the polarization of molecular angular momenta), which has to be compared to the experimental value 0.028.

The third reason indicated by Monchick, Munn and Mason [42]) for the failure of the previous calculations, is that it may not be allowed to take degeneracy averaged cross sections, as shown by McCourt and Snider [12]). Using the ideas of Kagan and Maksimow [52]) these authors took into account the possibility of an anisotropic angular momentum distribution of the rotating molecules. But the corrections arising from this modification of the treatment will also not be sufficient, as is shown in the recent paper by Sandler and Dahler [53]). It amounts to only 15 % of the value which they obtained with the loaded sphere model.

The phenomenological treatment of the problem in the first two sections of

this paper indicates that another generalization of the Boltzmann equation must first be performed. The production of particles of a component, due to the reactions in the multicomponent mixture, has not been taken into account in the derivation. We can state this more precisely by a comparison between the macroscopic entropy production, and the entropy production derivable from the kinetic theory. The two should be identical in the first approximation of Chapman and Enskog. Thermodynamics of irreversible processes give the following formula (ref. 43, p. 181) for the entropy production of reacting mixtures in which concentration gradients may build up and a thermal gradient is applied:

$$\sigma = \vec{J}_q \cdot \operatorname{grad} \frac{1}{T} - \sum_{i=1}^{n} \vec{J}_i \cdot \operatorname{grad} \frac{\mu_i}{T} - \frac{1}{T} \sum_{j=1}^{r} J_j A_j , \tag{3.33}$$

where J_j and A_j are the reaction rates and the affinities which characterize the r reactions. $\vec{J}_q$ is the heat flux. The last term of (3.33) is missing in the entropy source strength, derived from the kinetic equations of the authors mentioned [10, 12, 48]. For the same reason the balance equation for each individual component has to be extended with a source term, expressing the production or destruction of the component over all reactions

$$\frac{\partial \rho_i}{\partial t} = - \operatorname{div} \rho_i \vec{v}_i + \sum_{j=1}^{r} \nu_{ij} J_j . \tag{3.34}$$

Because of the conservation of mass in every chemical reaction the coefficients of the reaction equation, ν_{ij}/M_i, have to vanish according to

$$\sum_{i=1}^{n} \nu_{ij} = 0. \tag{3.35}$$

Therefore, the law of total mass conservation stays the same

$$\frac{\partial \rho}{\partial t} = - \operatorname{div} \rho \vec{v}. \tag{3.36}$$

The discrepancy arises in the transition from the Boltzmann equations for the individual components, which may be the internal states (leaving out external forces)

$$\frac{\partial f_i}{\partial t} = - \vec{v}_i \cdot \frac{\partial f_i}{\partial \vec{r}} + \sum_{j=1}^{n} C (f_i, f_j) ; \quad (i = 1, \ldots, n - 1) \tag{3.37}$$

to the Boltzmann equation of the system as a whole, i.e. in our calculations the binary mixture of α and β. In (3.37) the collision term $C(f_i, f_j)$ now contains a part which accounts for the change in the number of i-particles, becoming j-particles, due to inelastic collisions. The summational property of the collision term part is no longer invariant for the properties ψ_i, which are concerned in the chemical reaction

$$\sum_{i,j}^{n} \int \psi_i \, C(f_i, f_j) \, d\vec{v}_i \neq 0, \tag{3.38}$$

for instance for ψ_i being the internal energy or the angular momentum of the molecule.

$$\sum_{j=1}^{n} \int C(f_i, f_j) \, d\vec{v}_i = b_i \neq 0 \tag{3.39}$$

is now the non-vanishing number of molecules i produced per unit time and per unit volume by all the transitions. Therefore

$$\sum_{i=1}^{n-1} \frac{\partial f_i}{\partial t} \neq \frac{\partial f_\alpha}{\partial t} \tag{3.40}$$

It now seems important to us to proceed with the solution of this new type of Wang Chang - Uhlenbeck equation in order to obtain kinetic expressions of the diffusion and thermal diffusion coefficients, preserving the terms which depend on the rates of transition between the internal states. These will provide a rigorous check for the expressions obtained in our theory.

3.6 CONCLUSIONS

In order to avoid a rather laborious extension of the treatment of Wang Chang, Uhlenbeck and De Boer [9]) to mixtures where the rate of transition between translational and internal energy is slow with respect to the establishment of kinetic equilibrium, we developed a phenomenological treatment based on thermodynamics of irreversible processes. We made use of the concept, which considers the internal degrees of freedom as chemical components reacting among each other. Thus we were able to introduce new expressions in diffusion and thermal diffusion coefficients, which account for the production of components in a system, when simultaneously undergoing gradients in the concentration

and in temperature. We could confine the expressions to the chemical equilibrium case between the internal states, because from the macroscopic point of view local equilibrium is maintained, the rate of energy exchange being still rapid with respect to the establishment of hydrodynamic equilibrium.

The second feature of the problem which we took into account is that the macroscopic measurement cannot discern between the different internal states. The transition of the multicomponent system of reacting internal species to a quasi binary system is, however, not a simple summation. We indicated the way to make this transition in both kinetic and phenomenological theories.

The actual calculation of the transport coefficients from our theory requires the insertion of the simple kinetic expressions for the binary diffusion coefficients in a multi component mixture or the simple collision integrals for which we chose the expressions derived by Waldmann [14]). We applied our theory to the evaluation of the diffusion coefficient and the thermal diffusion factor of the He - HT mixture. The HT molecules have rotational degrees of freedom and an asymmetric mass distribution. Therefore the transport cross sections for elastic scattering on which the collision integrals depend have to be calculated with a potential model as realistic as possible. This was performed in section 2.5, where an inelastic formula was used in order to take proper account of every contribution to the displacement in the scattering, but the transition probabilities in HT at room temperature are so small that the cross sections are close to the elastic limit.

The agreement with experiments is much improved as compared to earlier attempts.

REFERENCES

1. E.A. Mason, I. Amdur and I. Oppenheim, J.Chem.Phys. 43, 4458 (1965).
2. E.A. Mason, R.J. Munn and F.J. Smith, "Advances in Atomic and Molecular Physics" 2, 33 (1966).
3. J. Schirdewahn, A. Klemm and L. Waldmann, Z.Naturf. 16a, 133 (1961).
4. W. Reichenbacher and A. Klemm, Z.Naturf. 19a, 1051 (1964).
5. V. Boersma-Klein and A.E. de Vries, Physica 32, 717 (1966).
6. K. Clusius and P. Flubacher, Helv.Chim.Acta 41, 2323 (1958).
7. H.F.P. Knaap and J.J.M. Beenakker, Physica 27, 523 (1961).
8. S. Chapman and T.G. Cowling, "The Mathematical Theory of Non-uniform Gases" (Cambridge, 1939).
9. C.S. Wang Chang, G.E. Uhlenbeck and J. de Boer, "Studies in Statistical Mechanics" (New York, 1964) 2, 241.
10. L. Monchick, K.S. Yun and E.A. Mason, J.Chem.Phys. 39, 654 (1963).
11. L. Waldmann, "Statistical Mechanics of Equilibrium and Non-equilibrium", ed. J. Meixner, (Amsterdam, 1965), p. 177.
12. F.R. McCourt and R.F. Snider, J.Chem.Phys. 41, 3185 (1964); 43, 2276 (1965).
13. F. v.d. Valk, thesis (Amsterdam, 1963); M.F. Laranjeira, thesis (Leiden, 1959).
14. L. Waldmann, Handb.Phys. 12, 436 (1958).
15. E.W. Becker and W. Beyrich, J.Chem,Phys. 56, 911 (1952).
16. C.J.G. Slieker, thesis (Amsterdam, 1964).
17. B.F. Murphey, Phys.Rev. 72, 836 (1947).
18. E. Trübenbacher, Z.Naturf. 17a, 539 (1962).
19. T. Kihara, "Imperfect Gases" (Tokyo, 1949).
20. J.O. Hirschfelder, C.F. Curtiss and R.B. Bird, "Molecular Theory of Gases and Liquids" (New York, 1954), Chap. 7 and 8.
21. E.A. Mason, J.Chem.Phys. 27, 75 (1957).
22. T. Kihara, Rev.Mod.Phys. 25, 839 (1953).
23. E.A. Mason and W.E. Rice, J.Chem.Phys. 22, 522 (1954).
24. E.A. Mason, J.Chem.Phys. 22, 169 (1954).
25. J.A. Barker, W. Fock and F. Smith, Phys.Fluids 7, 897 (1964).
26. W. Reichenbacher, P. Müller and A. Klemm, Z.Naturf. 20a, 1529 (1965).
27. S. Imam-Rahajoe, C.F. Curtiss and R.B. Bernstein, J.Chem.Phys. 42, 530 (1965);
    R.J. Munn, F.J. Smith, E.A. Mason and L. Monchick, J.Chem.Phys. 42, 537 (1965).
28. A.E. de Vries and A. Haring, Z.Naturf. 20a, 433 (1965).

29. H. van Ee, thesis (Leiden, 1966).

30. E.A. Mason, M. Islam and S. Weismann, Phys. Fluids 7, 1011 (1964).

31. K. Takayanagi, Suppl. Progr. Theor. Phys. 25, 1 (1963).

32. A.M. Arthurs and A. Dalgarno, Proc. Roy. Soc. A256, 540 (1960).

33. C.S. Roberts, Phys. Rev. 131, 203, 209 (1963).

34. W.D. Davison, Disc. Far. Soc. 33, 71 (1962).

35. C.G. Sluijter, thesis (Leiden, 1964).

36. R.J. Cross and D.R. Herschbach, J. Chem. Phys. 43, 3530 (1965).

37. E.T. Whittaker, "Analytical Dynamics of Particles and Rigid Bodies", (Cambridge, 1964), Chap. 13.

38. A.M. Arthurs and J.T. Lewis, Proc. Roy. Soc. A269, 585 (1962).

39. J.A. Zonneveld, "Automatic Numerical Integration", Mathematical Centre Tracts n° 8 (Amsterdam, 1964).

40. I. Amdur and J.W. Beatty, J. Chem. Phys. 42, 3361 (1965).

41. N. Taxman, Phys. Rev. 110, 1235 (1958).

42. L. Monchick, R.J. Munn and E.A. Mason, J. Chem. Phys. 45, 3051 (1966).

43. S.R. de Groot and P. Mazur, "Non-equilibrium Thermodynamics" (Amsterdam, 1962), p. 284.

44. I. Prigogine and P. Mazur, Physica 19, 241 (1953).

45. J. Meixner, Z. Naturf. 8a, 69 (1953).

46. I. Prigogine and R. Buess, Acad. Roy. Belg., Bull. Cl. Sc. 38, 711, 851 (1952).

47. P.A.M. Dirac, Proc. Cambr. Phil. Soc. 22, 132 (1925); W. Nernst, Boltzmann Festschrift 904 (1904).

48. L. Waldmann and E. Trübenbacher, Z. Naturf. 17a, 363 (1962).

49. J. van de Ree, Physica, in course of publication.

50. B. Baranowski and J. van de Ree, Physica 31, 1428 (1965).

51. S.I. Sandler and J.S. Dahler, J. Chem. Phys. 44, 1229 (1966); 43, 1750 (1965).

52. Yu. Kagan and L. Maksimov, Zh. Eksperim. i Teor. Fiz. 41, 842 (1961), English translation: Soviet Phys. - JETP 14, 604 (1962).

53. S.I. Sandler and J.S. Dahler, to be published.

SUMMARY

The thermal diffusion factors α for small concentrations of all possible hydrogen isotopes in inert gases were measured between 100 ^{o} C and 600 ^{o}C, and compared with the values from the Chapman - Enskog theory. It appeared that a Buckingham exp.-6 potential model with parameters derived from measured viscosity and second virial coefficients could fit the separations of the symmetric molecules H_2, D_2 and T_2. It was, however, impossible to fit the values of the asymmetric molecules HD, HT and DT into this theory. An analysis of possible sources of deviations, such as higher order approximations, quantum corrections or inelastic collisions indicated no way to improve the theoretical values. The overall behaviour is thus very similar to that found in mutual thermal diffusion of hydrogen isotopes. In Chapter 1 an empirical formula was derived which could describe the series of experiments with the lighter inert gases. This formula suggested a linear dependence of the deviations on the displacement of the centre of mass of the colliding system.

Focussing our attention on the deviation between the thermal diffusion factors of ^{4}He-D_2 and ^{4}He-HT, we have calculated the cross sections for inelastic scattering of the ^{4}He atom in collisions with the HT molecule considered as a rigid rotator. The set of coupled differential equations arising from the classical mechanical formulation of the three body collision problem was solved numerically. We introduced the rotating potential model, involving a potential field spherically symmetric about the geometrical midpoint of the molecule, which rotates around its centre of mass. The results show large deviations from the cross sections obtained with a simple non-eccentric spherical potential. These deviations depend strongly on the orientation and the angular momentum $\vec{J}$ of the molecule. An analysis of the effect of the space orientation of $\vec{J}$ reveals a considerable polarization. A reasonable approximation to an orientation averaged

cross section can be obtained by taking the position of $\vec{J}$ perpendicular to the collision plane as representative, which permits simplification to a two-dimensional collision calculation. There is a positive increase in the cross section which can be as much as 20 % for low relative velocities and high values of J. It is possible to calculate the probability for change of the rotational state, showing how correctly a calculation based on classical mechanics can describe a quantum phenomenon. The new calculations predict an increase in the transition probabilities from 10^{-3} to about 5. 10^{-2}. This is in accordance with the value expected from experiments.

In order to avoid a rather laborious extension of the treatment of Wang Chang, Uhlenbeck and De Boer to mixtures where the rate of exchange between translational and internal energy is slow, we developed a phenomenological treatment based on thermodynamics of irreversible processes. We introduced new expressions for the thermal diffusion and diffusion coefficients which account for this exchange in the case of a local equilibrium distribution between the rotational states of HT. We made use of the concept in which the internal degrees of freedom are considered as chemically reacting components. The multicomponent diffusion coefficients occurring in the new expressions were related to the newly calculated collision integrals based on the transport cross sections obtained in Chapter 2. The agreement between the theoretical diffusion and thermal diffusion coefficients and the experiments for a ^{4}He-HT mixture is much improved as compared to earlier attempts.

SAMENVATTING

In het eerste hoofdstuk worden metingen vermeld van de thermodiffusiefactor α tussen 100^{o} en 600^{o} Celsius voor mengsels van edelgassen en kleine concentraties van alle bestaande waterstof isotopen. De resultaten worden vergeleken met de waarden uit de theorie van Chapman en Enskog. De grootste overeenstemming wordt bereikt door het gebruik van de Buckingham exp.-6 potentiaal met parameters verkregen uit metingen van de viscositeit en de tweede viriaal coefficient. Dit geldt voor de symmetrische moleculen H_2, D_2 en T_2, maar het blijkt onmogelijk de waarden van de asymmetrische moleculen HD, HT en DT op deze wijze te verklaren. Correcties voor hogere orde effecten, quantum-effecten of inelastische botsingen, brengen hierin geen verbetering. Dezelfde problemen doen zich voor bij de thermodiffusie van mengsels van waterstof isotopen onderling. Wij hebben een empirische formule opgesteld, die in staat is de waarden van de mengsels met lichte edelgassen redelijk te beschrijven. Deze formule wijst in de richting van een lineair verband met de verlegging van het massazwaartepunt in het systeem van de botsende deeltjes.

Wij hebben ons voor het vervolg beperkt tot het verschil tussen de thermodiffusie factor van ^{4}He-D_2 en ^{4}He-HT mengsels. Daartoe hebben wij in hoofdstuk 2 de botsingsdoorsneden berekend, die optreden bij de inelastische botsingen tussen het ^{4}He atoom en het HT molecule, opgevat als starre rotator. Uit de klassieke mechanica volgt een stelsel van gekoppelde differentiaal vergelijkingen, die dit drie deeltjes probleem beschrijven. Dit stelsel werd numeriek opgelost met behulp van een rekenautomaat. Om de wisselwerking te beschrijven, hebben wij een roterend potentiaal model ontworpen, dat bestaat uit een bolsymmetrische potentiaal waarvan het centrum ligt in het meetkundig middelpunt van het molecule, dat op zijn beurt draait om het massazwaartepunt. Wij vonden grote afwijkingen in de botsingsdoorsneden vergeleken met die, waarvoor een bolsym-

metrische potentiaal zonder meer was gebruikt. Deze afwijkingen hangen sterk af van de orientatie en van het impulsmoment $\vec{J}$ van het molecule en vertonen polarisatie, afhankelijk van de stand van $\vec{J}$ in de ruimte. Het gemiddelde van de beide standen van $\vec{J}$ loodrecht op het vlak van botsing, vormt een goede benadering. De berekeningen vereenvoudigen dan tot een twee-dimensionale baanberekening. Voor lage relatieve snelheden en hoge waarden van J, zijn de diffusie botsingsdoorsneden 20% hoger dan vroeger. Wij kunnen ook overgangswaarschijnlijkheden berekenen tussen de rotatie toestanden door een kunstmatige grens tussen de energie niveau's aan te nemen. Het is dan opmerkelijk dat klassiek mechanische berekeningen een dergelijk quanteus verschijnsel goed kunnen benaderen. De overgangswaarschijnlijkheden in HT zijn van de orde 5.10^{-2}, te vergelijken met 10^{-3} voor D_2. Deze getallen stemmen overeen met wat experimenteel te verwachten is.

Een passende kinetische theorie voor de transport verschijnselen in een mengsel van ^{4}He en HT, zou gevonden moeten worden door de theorie van Wang Chang, Uhlenbeck en de Boer uit te breiden tot mengsels waarin de overdracht tussen kinetische energie en de energie van de inwendige vrijheidsgraden langzaam verloopt. In plaats daarvan hebben wij in hoofdstuk 3 een phenomenologische behandeling van het probleem verkozen aan de hand van de thermodynamica van irreversibele processen. Daarbij vonden wij nieuwe uitdrukkingen voor de thermodiffusie en diffusie coefficienten, die deze uitwisseling in rekening brengen. Wij konden ons beperken tot het geval van plaatselijk evenwicht tussen de rotatie toestanden van HT. Hierbij zijn de interne vrijheidsgraden opgevat als chemisch reagerende componenten. In de nieuwe uitdrukkingen komen multicomponente diffusie coefficienten voor, die wij in verband gebracht hebben met de kinetische botsingsintegralen en de diffusie botsingsdoorsneden, die in het tweede hoofdstuk werden berekend. De overeenstemming tussen de theoretische en experimentele thermodiffusie factoren en diffusie coefficienten van het He-HT mengsel, is nu veel beter geworden.

DANKWOORD

Gaarne wil ik van deze gelegenheid gebruik maken allen te bedanken die hebben bijgedragen aan de totstandkoming van dit proefschrift.

De samenwerking met Dr. J. Los en Dr. A.E. de Vries is hierbij van primair belang geweest. De gelegenheid om met anderen van gedachten te wisselen is een onmisbare schakel in de totstandkoming van wetenschappelijke resultaten. Die gelegenheid is mij door het F.O.M. - Instituut voor Atoom- en Molecuulfysica in ruime mate geboden. Gaarne wil ik hier de namen noemen van Dr. E.G.D. Cohen, Dr. M.J. Offerhaus, Dr. G.E. Uhlenbeck, Dr. B. Baranowski en Drs. A. Tip.

De medewerkers van de Groep Molecuulfysica hebben mij bijzonder geholpen door zeer veel van het experimentele werk van mij over te nemen, toen dit eenmaal het stadium van routineonderzoek bereikt had. Hierbij hebben Mej. J. Westmijze en Mej. A. Tom blijk gegeven van grote zelfstandigheid, zodat ik mijn handen vrij kreeg voor het meer theoretische deel van dit werk. H. v.d. Brink verdient bijzondere vermelding voor het verrichten van de talloze massaspectrometrische analyses. Bij de constructie van een apparaat voor het differentieel meten van de temperatuurafhankelijkheid van de thermodiffusiefactor, heb ik veel te danken gehad aan de assistentie van E. Keur en A. Haring, aan de electronische afdeling onder leiding van P.J. van Deenen, in het bijzonder van W. Tebra, aan de werkplaats onder leiding van A.F. Neuteboom, aan de glasblazerij onder leiding van J.A. van Wel, aan de vacuumafdeling onder J.C. Heyboom.

Gaarne wil ik de Wiskundige Dienst van de Technische Hogeschool in Delft danken voor het uitvoeren van een deel van de berekeningen op de rekenautomaat TR-4, in het bijzonder Ir. L.B.D. Harkema voor zijn voortreffelijke assistentie. Ook de staf van het Mathematisch Centrum in Amsterdam wil ik mijn erkentelijk-

heid betuigen voor het uitvoeren van het tweede deel van de berekeningen, vooral toen dit in nachtwerk is uitgelopen. Dr. Th. J. Dekker wil ik danken voor zijn hulp bij het programmeren. Mej. A. Tom en H. Drion hebben geholpen bij de uitwerking van de resultaten. Dr. D. Vroom en Dr. D. Gibson dank ik voor het corrigeren van dit proefschrift op de ergste fouten in de Engelse taal.

Verder wil ik Mej. M.J. Benavente danken voor het vervaardigen van de tekeningen, F.L. Monterie en Th. van Dijk voor het fotografisch werk, Mej. J.M. de Vletter voor het typen van het manuscript, en Mej. A. Klapmuts voor algemene hulp bij administratieve problemen.

Naast de dank voor al deze hulp bij de fysische opbouw van dit proefschrift, past een eervolle vermelding voor mijn vrouw, die het psychische steigerwerk verzorgd heeft.

STELLINGEN

1

Sinha en Müller hebben in een veldionen-microscoop beschadigingen waargenomen aan het oppervlak van Wolfram-kristallen bij beschieting met Helium atomen van 20 keV. Hun conclusies over de oorzaak van de roosterdefecten en de lengte van de focusserende stoten serie zijn echter niet consistent.

M.K. Sinha en E.W. Müller, J. Appl. Phys. 35 (1964) 1256.

2

De verwachting van Martin et al., dat bij het ionisatieproces bij hoge botsingsenergieën (> 1 MeV) He^+ opgevat kan worden als een projectiel met effectieve lading $1 < Z_{eff} < 2$, is theoretisch onjuist.

D.W. Martin, R.A. Langley, D.S. Harmer, J.W. Hooper en E.W. McDaniel, Phys. Rev. 136 (1964) A 385.

3

De door Gibson et al. gemeten anomalie t.o.v. de theoretische Born-benadering in de hoekafhankelijkheid van de door botsingen met atomen geïnduceerde excitatie van H_2^+ ionen, duidt op de vorming van een intermediair botsingscomplex met het doelwit atoom.

G.W. McClure, Phys. Rev. 140 (1965) A 769;
D.K. Gibson, J. Los en J. Schopman, Vth International Conference on the Physics of Electronic and Atomic Collisions, Abstracts of Papers (Publ. House NAUKA, Leningrad 1967) p.594;
G.H. Dunn, Phys. Rev. Letters 8 (1962) 62.

4

De interpretatie die door Yates en Garland wordt gegeven van het infrarood spectrum van koolmonoxyde, gechemisorbeerd op nikkel-catalysatoren, is onvolledig en gedeeltelijk onjuist.

J.T. Yates en C.W. Garland, J. Phys. Chem. 65 (1961) 617.

5

Bij de interpretatie van N.M.R. spectra van geprotoneerde, asymmetrisch gesubstitueerde benzophenonen is de mogelijkheid van belemmerde rotatie om de C-O binding ten onrechte buiten beschouwing gelaten.

Th.J. Sekuur en P. Kranenburg, Tetrahedron Letters 1966, 4793.

6

Het optreden van ionen als tussenproduct in de reactie tussen alkali atomen en halogeen moleculen, kan worden bewezen met atomaire bundel-apparatuur in het eV gebied.

D.R. Herschbach, Advances of Chem. Phys. 10 (1966) 319.

7

De berekeningen van Cross en Herschbach voor de strooiing van een atoom aan een starre rotator zijn misleidend en waarschijnlijk foutief, omdat te weinig aandacht is geschonken aan de betekenis van het geïnduceerde impulsmoment.

R.J. Cross en D.R. Herschbach, J. Chem. Phys. 43 (1965) 3530.

8

Het falen van de theorie van Monchick en Mason in de berekening van de thermodiffusiefactoren van mengsels van edelgas-atomen en meeratomige moleculen van ongeveer dezelfde massa, berust op meer ingrijpende gronden dan de door de auteurs genoemde oorzaken.

L. Monchick, K.S. Yun en E.A. Mason, J. Chem. Phys. 39 (1963) 654;
L. Monchick, R.J. Munn en E.A. Mason, J. Chem. Phys. 45 (1966) 3051;
dit proefschrift.

9

In de toelichting op de prijsvraag van Teyler's Genootschap van dit jaar is de definitie van typografische poëzie niet adequaat.

Prijsvraagprogramma van Teyler's Tweede Genootschap te Haarlem (1 januari 1967).

10

Naarmate de technische mogelijkheden in de verschillende experimentele gebieden zich uitbreiden, verliest de fysica steeds meer van haar empirisch karakter.

J. van de Ree

oktober 1967.